LI
LABORATORY INVESTIGATION
THE BASIC AND TRANSLATIONAL PATHOLOGY RESEARCH JOURNAL
VOLUME 99 | SUPPLEMENT 1 | MARCH 2019

USCAP 2019

ABSTRACTS

PEDIATRIC PATHOLOGY (1771-1802)

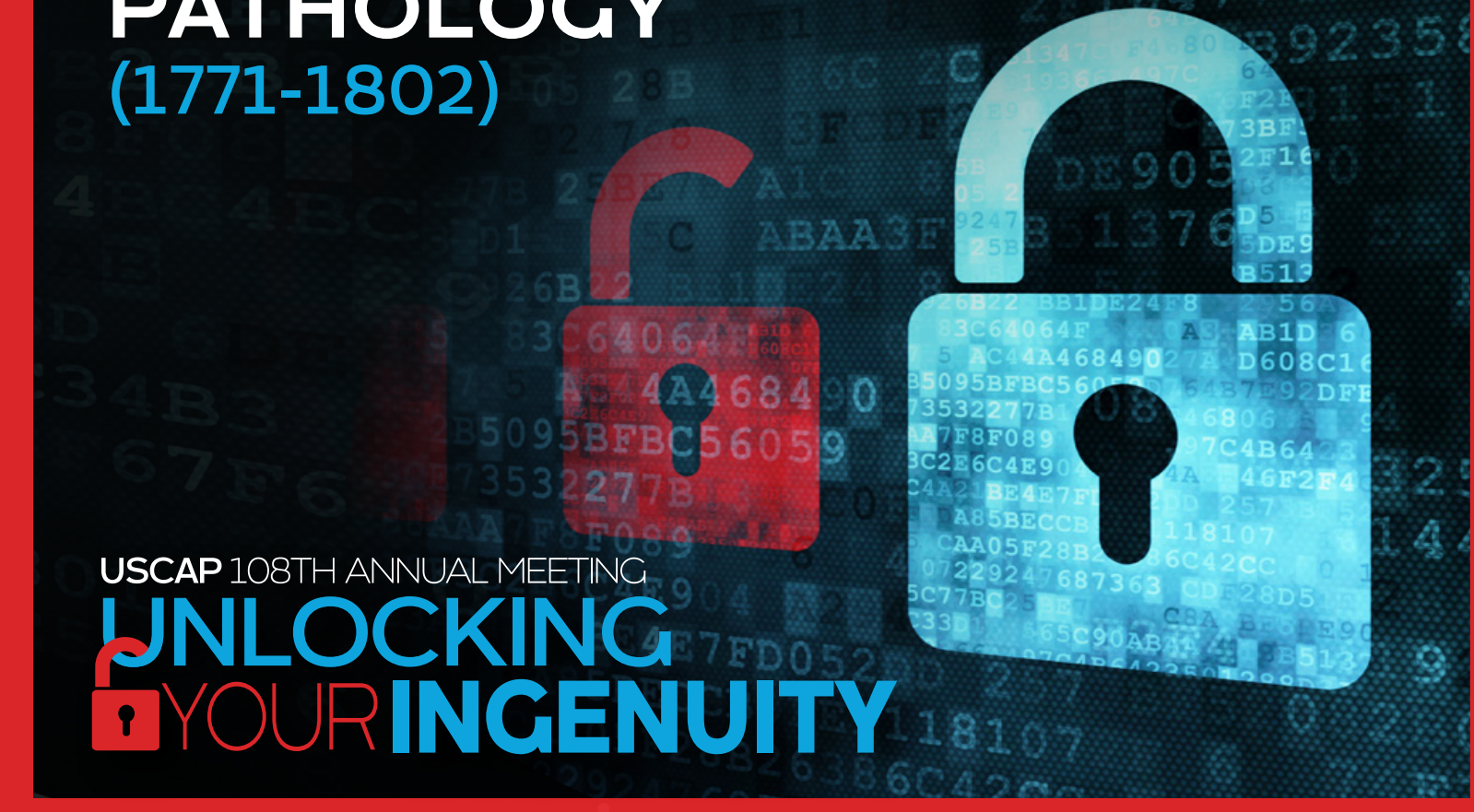

USCAP 108TH ANNUAL MEETING

UNLOCKING YOUR INGENUITY

MARCH 16-21, 2019

National Harbor, Maryland
Gaylord National Resort & Convention Center

Published by
SPRINGER NATURE
www.ModernPathology.org

USCAP Creating a Better Pathologist
AN OFFICIAL JOURNAL OF THE UNITED STATES AND CANADIAN ACADEMY OF PATHOLOGY

EDUCATION COMMITTEE

Jason L. Hornick, Chair
Rhonda K. Yantiss, Chair, Abstract Review Board and Assignment Committee
Laura W. Lamps, Chair, CME Subcommittee
Steven D. Billings, Interactive Microscopy Subcommittee
Shree G. Sharma, Informatics Subcommittee
Raja R. Seethala, Short Course Coordinator
Ilan Weinreb, Subcommittee for Unique Live Course Offerings
David B. Kaminsky (Ex-Officio)
Aleodor (Doru) Andea
Zubair Baloch
Olca Basturk
Gregory R. Bean, Pathologist-in-Training
Daniel J. Brat
Ashley M. Cimino-Mathews
James R. Cook
Sarah M. Dry
William C. Faquin
Carol F. Farver
Yuri Fedoriw
Meera R. Hameed
Michelle S. Hirsch
Lakshmi Priya Kunju
Anna Marie Mulligan
Rish Pai
Vinita Parkash
Anil Parwani
Deepa Patil
Kwun Wah Wen, Pathologist-in-Training

ABSTRACT REVIEW BOARD

Benjamin Adam
Michelle Afkhami
Narasimhan (Narsi) Agaram
Rouba Ali-Fehmi
Ghassan Allo
Isabel Alvarado-Cabrero
Christina Arnold
Rohit Bhargava
Justin Bishop
Jennifer Boland
Elena Brachtel
Marilyn Bui
Shelley Caltharp
Joanna Chan
Jennifer Chapman
Hui Chen
Yingbei Chen
Benjamin Chen
Rebecca Chernock
Beth Clark
James Conner
Alejandro Contreras
Claudiu Cotta
Timothy D'Alfonso
Farbod Darvishian
Jessica Davis
Heather Dawson
Elizabeth Demicco
Suzanne Dintzis
Michelle Downes
Daniel Dye
Andrew Evans
Michael Feely
Dennis Firchau
Larissa Furtado
Anthony Gill
Ryan Gill
Paula Ginter
Tamara Giorgadze
Raul Gonzalez
Purva Gopal
Anuradha Gopalan
Jennifer Gordetsky
Rondell Graham
Alejandro Gru
Nilesh Gupta
Mamta Gupta
Krisztina Hanley
Douglas Hartman
Yael Heher
Walter Henricks
John Higgins
Mai Hoang
Mojgan Hosseini
Aaron Huber
Peter Illei
Doina Ivan
Wei Jiang
Vickie Jo
Kirk Jones
Neerja Kambham
Chiah Sui (Sunny) Kao
Dipti Karamchandani
Darcy Kerr
Ashraf Khan
Rebecca King
Michael Kluk
Kristine Konopka
Gregor Krings
Asangi Kumarapeli
Alvaro Laga
Cheng-Han Lee
Zaibo Li
Haiyan Liu
Xiuli Liu
Yan-Chun Liu
Tamara Lotan
Anthony Magliocco
Kruti Maniar
Jonathan Marotti
Emily Mason
Jerri McLemore
Bruce McManus
David Meredith
Anne Mills
Neda Moatamed
Sara Monaco
Atis Muehlenbachs
Bita Naini
Dianna Ng
Tony Ng
Ericka Olgaard
Jacqueline Parai
Yan Peng
David Pisapia
Alexandros Polydorides
Sonam Prakash
Manju Prasad
Peter Pytel
Joseph Rabban
Stanley Radio
Emad Rakha
Preetha Ramalingam
Priya Rao
Robyn Reed
Michelle Reid
Natasha Rekhtman
Michael Rivera
Michael Roh
Andres Roma
Avi Rosenberg
Esther (Diana) Rossi
Peter Sadow
Safia Salaria
Steven Salvatore
Souzan Sanati
Sandro Santagata
Anjali Saqi
Frank Schneider
Jeanne Shen
Jiaqi Shi
Wun-Ju Shieh
Gabriel Sica
Deepika Sirohi
Kalliopi Siziopikou
Lauren Smith
Sara Szabo
Julie Teruya-Feldstein
Gaetano Thiene
Khin Thway
Rashmi Tondon
Jose Torrealba
Evi Vakiani
Christopher VandenBussche
Sonal Varma
Endi Wang
Christopher Weber
Olga Weinberg
Sara Wobker
Mina Xu
Shaofeng Yan
Anjana Yeldandi
Akihiko Yoshida
Gloria Young
Minghao Zhong
Yaolin Zhou
Hongfa Zhu
Debra Zynger

1771 Perinatal pulmonary hemorrhage: A retrospective autopsy case series

Indu Agarwal[1], Linda Ernst[2]
[1]Northshore University, Evanston, IL, [2]University of Chicago at NorthShore HealthSystem, Evanston, IL

Disclosures: Indu Agarwal: None; Linda Ernst: None

Background: Perinatal pulmonary hemorrhage (PH) is a condition characterized by blood loss via the respiratory tract, often with concomitant respiratory distress and clinical deterioration. It has an incidence of approximately 0.1% in all newborns, but this increases to 5-11% in preterm infants or infants with mortality rates between 38-68%. The anatomical/histologic characteristics of the lung in PH are not well characterized, and we hypothesized that pulmonary maldevelopment such as pulmonary hypoplasia may contribute to PH. In addition, we sought to find any correlations with placental pathology.

Design: Fetal and neonatal autopsies with diagnosis of PH were retrieved from Pathology database between 2009-2015. Autopsy reports were reviewed. Demographic data and gross data regarding lung sizes and weights were collected. H&E sections of the lung autopsy slides were retrieved and PH was graded based on involvement of lung tissue. The stage of lung development, radial alveolar count, and persistence of intra-acinar arterioles were also assessed. Placental pathology reports were also retrieved for each case and reviewed.

Results: 17 cases were identified meeting inclusion criteria. 9 were stillborn and 8 were live born. Gestational ages at birth range from 23.5 to 40.5 weeks gestation and the male to female ratio was 6:11. 4/17 (23.5%) had major congenital anomalies and 1/17 (5.8%) had an abnormal karyotype (69,XXX). PH ranged from mild (<5% in each lung) to severe (>75% in both lungs) (table 1). There were 6 cases in which PH involved >50% of both lungs. Lung to body weight ratios ranged from 0.006 to 0.288 with pulmonary hypoplasia designated in 7/17 (41.17%) cases with PH. Pulmonary hypoplasia and/or persistence of intra-acinar arterioles was seen in 13/17 (76.4%) of cases.

No specific placental pathology was seen universally in the cases of PH, but the placental weight <10th percentile was seen in 10/17 (59%) of the cases and evidence of either maternal or fetal vascular malperfusion was present in 13/17 (76%) of the PH cases. Umbilical cord abnormalities were present in 8/17 (47%) of PH cases, and acute inflammation was present in 9/17 (53%) of PH cases.

Table 1: Summary of pulmonary findings in cases of pulmonary hemorrhage.

Case	PH right lung (%)	PH left lung (%)	Developmental Stage	Radial aveolar count	Intra acinar arterioles	Combined Lung weight (g)	Lung/body weight ratio	pulmonary hypoplasia
A	<5	<5	Aveolar	4	no	57.36, AGA	0.02 (WNL)	no
B	<5	<5	Saccular	3	yes	7.63, SGA	0.006 (BNL)	yes
C	5 -- 25	<5	Aveolar	4	no	54.75, AGA	0.0167 (WNL)	no
D	5 -- 25	<5	Saccular	2	yes	26.92, AGA	0.017 (BNL)	yes
E	5 -- 25	5 -- 25	Saccular	2	no	18.45, AGA	0.288 (WNL)	no
F	5 -- 25	5 -- 25	Aveolar	4	yes	45.23, AGA	0.0264 (WNL)	no
G	5 -- 25	5 -- 25	Aveolar	3	yes	53.14, AGA	0.017 (BNL)	yes
H	25 -- 50	5 -- 25	Saccular	2	no	15, AGA	0.031 (WNL)	no
I	>75	<5	Aveolar	4	no	44.74, AGA	0.011 (BNL)	yes
J	25 -- 50	25 -- 50	Saccular	2	yes	46, LGA	0.032 (ANL)	no
K	25 -- 50	25 -- 50	Aveolar	4	yes	69.5, LGA	0.02 (WNL)	no
L	50 -- 75	50 -- 75	Saccular	1	no	14.28, SGA	0.007 (BNL)	yes
M	>75	50 -- 75	Aveolar	5	yes	38.15, AGA	0.013 (WNL)	no
N	>75	50 -- 75	Aveolar	3	yes	112, LGA	0.025 (WNL)	no
O	>75	>75	Saccular	2	no	4.21, SGA	0.007 (BNL)	yes
P	>75	>75	Aveolar	2	yes	60.74, AGA	0.017 (BNL)	yes
Q	>75	>75	Aveolar	3	yes	66, LGA	0.02 (WNL)	no

PH = Pulmonary hemorrhage, WNL = Within normal limits, BNL = Below normal limits, ANL = Above normal limits, g = grams,

AGA = appropriate for gestational age, LGA = large for for gestational age, SGA = small for for gestational age, Y = yes, N = no

Conclusions: Our data suggests that PH may be associated with pulmonary maldevelopment and that the pulmonary hypoplasia and persistence of intra-acinar arterioles may be features of lungs with PH. While no specific placental pathology is seen in PH, maternal and fetal vascular pathology is common.

1772 Helicobacter pylori-Associated Inflammatory Infiltrates in Children

Nadine Aguilera[1], Jennifer Ju[2], Mani Mahadevan[3], Jinbo Fan[2], Edward Stelow[2]
[1]University of Virginia Health System, Fredericksburg, VA, [2]University of Virginia Health System, Charlottesville, VA, [3]University of Virginia, Charlottesville, VA

Disclosures: Nadine Aguilera: None; Jennifer Ju: None; Mani Mahadevan: None; Jinbo Fan: None; Edward Stelow: None

Background: Helicobacter pylori (HP) infection is uncommon in children in the US but has a higher incidence in developing countries. In children, the associated lymphocytic infiltrate is less alarming than in adults due to the higher frequency of general lymphoid hyperplasia and rarity of marginal zone lymphoma of mucosa associated lymphoid tissue (MALT lymphoma). HP is considered a major predisposing factor for MALT lymphoma in adults, possibly due to the longer duration of chronic antigenic stimulation. There are few studies describing the inflammatory infiltrates associated with HP in children.

Design: Sixty-two HP positive (diagnosed on H&E or IHC) stomach biopsies in children (ages 0-18 years) were identified. The biopsies and foveolar fragments were assessed for strength (0-25%, 26-50%, 51-75%, or 76-100% stromal presence), linear spread (patchy or diffuse), depth (superficial or full-thickness), activity, composition of inflammation within the lamina propria (LP) (% of neutrophils, lymphocytes, plasma cells, or eosinophils), and presence of germinal centers (GC). The cases were scored by a modified Wotherspoon criteria (MWC) (scale 0-5). Twenty-two pediatric cases of moderate chronic gastritis which were HP negative by IHC were used for comparison. Molecular studies for *IGH* were performed on cases with MWC of 3 or greater.

Results: HP positive cases were significantly more likely to show GC than controls (50% versus 23%; p=0.04) and significantly more likely to score 3-5 by the MWC (47% versus 18%; p=0.02). Additionally, they were more likely to show activity (47% versus 14%, p=0.01). There was no significant difference between HP positive cases versus HP negative cases regarding strength of infiltrate (50% versus 45% for >75%; p=0.8), linear spread (52% versus 55% for diffuse; p=1.0), depth (68% versus 55% for full-thickness; p=0.2), average percentage of lymphocytes (37% versus 31%; p=0.3), presence of neutrophils in LP (47% versus 29%; p=0.14), and presence of eosinophils in LP (66% versus 59%; p=0.6). Three (two MWC=5 and one MWC=4) of 16 tested HP positive biopsies showed clonal *IGH* rearrangements.

Conclusions: In children, HP positive inflammatory infiltrates of the stomach show different morphologic features than HP negative gastritis. HP positive cases are more likely to show activity, GC formation and higher MWC scores with associated lymphoepithelial lesions. Although rare cases of HP positive gastritis show *IGH* clonality, the clinical course is generally benign.

1773 Tyrosine Hydroxylase Immunohistochemistry is Useful in the Distinction of Neuroblastoma from Histologic Mimics

Corey Allard[1], Munir Tanas[2], Andrew Bellizzi[1]
[1]University of Iowa Hospitals and Clinics, Iowa City, IA, [2]Iowa City, IA

Disclosures: Corey Allard: None; Andrew Bellizzi: None

Background: Tyrosine hydroxylase (TH) catalyzes the conversion of L-tyrosine to L-3,4-dihydroxyphenylalanine (L-DOPA), the rate limiting step in catecholamine biosynthesis. We recently optimized TH immunohistochemistry (IHC) for a research collaborator studying the sympathetic innervation of the tubal gut. Some endocrine pathologists have advocated for TH as a positive IHC marker of pheochromocytoma/paraganglioma, in the differential diagnosis with adrenal cortical carcinoma, renal cell carcinoma, and other metastatic carcinomas. We hypothesized that TH would be a sensitive and specific neuroblastoma marker in the differential diagnosis with other small round blue cell tumors.

Design: TH IHC was performed on tissue microarrays (tumors arrayed as triplicate 1 mm cores) of the following tumors: 66 neuroblastic tumors (6 undifferentiated, 34 poorly differentiated, 10 differentiating, 10 ganglioneuroblastomas, 6 maturing ganglioneuromas), 38 Wilms tumors, 27 melanomas, 21 synovial sarcomas, 16 alveolar rhabdomyosarcomas, 14 embryonal rhabdomyosarcomas, 15 lymphoblastic lymphomas, 11 mesenchymal chondrosarcomas, 10 Ewing sarcomas, 10 olfactory neuroblastomas, 7 malignant peripheral nerve sheath tumors, 6 desmoplastic small round cell tumors, and 2 *BCOR*-rearranged sarcomas. Expression was evaluated for intensity (0-3+) and extent (0-100%), and an H-score (intensity*extent) was calculated. Two-tail Mann-Whitney tests were used with $p<0.05$ considered significant.

Results: TH was expressed by 63 of 66 (95%) neuroblastic tumors at a mean (median) H-score of 223 (270) in positive tumors. It was only expressed by 2 of 177 (1.1%) non-neuroblastic tumors: 1 Wilms tumor (H-score 10) and 1 desmoplastic small round cell tumor (H-score 3.33). Detailed expression data by neuroblastic tumor type are presented in the Table. Median H-scores of the undifferentiated and maturing ganglioneuroma groups appeared to be less than that for all positive neuroblastic tumors considered together, but only the comparison for maturing ganglioneuroma was significant (p values of 0.14 and 0.042).

Tumor Type	n	% Positive (any H-score)	% Positive (H-score >/= 100)	Mean (Median) H-score (if positive)
Undifferentiated	6	100%	50%	142 (138)
Poorly differentiated	34	94%	85%	242 (283)
Differentiating	10	90%	90%	271 (270)
Ganglioneuroblastoma	10	100%	80%	234 (280)
Maturing ganglioneuroma	6	100%	50%	108 (90)

Conclusions: TH is a highly sensitive and specific marker of peripheral neuroblastic tumors, including neuroblastoma. This reflects their sympathoadrenal lineage. Based on the results of this study, we have clinically deployed TH IHC as a neuroblastoma marker in the differential diagnosis of small round blue cell tumors.

1774 Pediatric Large B-Cell Lymphoma: Can Genetic Profiling Improve Treatment Options?

Le Aye[1], Ali Nael[2], Sandra Hudson[3], Dongliang Wang[3], Dolores Estrine[4], Karen Gentile[3], Ashley Hagiya[5], Ryan Schmidt[4], Matthew Hiemenz[4], Gordana Raca[4], Robert Hutchison[3], Matthew Oberley[4]
[1]University of Southern California, Alhambra, CA, [2]Children Hospital of Orange County, University of California Irvine, Orange, CA, [3]SUNY Upstate Medical University, Syracuse, NY, [4]Children's Hospital Los Angeles, Los Angeles, CA, [5]Keck School of Medicine of University of Southern California, Pasadena, CA

Disclosures: Le Aye: None; Ali Nael: None; Sandra Hudson: None; Dongliang Wang: None; Dolores Estrine: None; Karen Gentile: None; Ashley Hagiya: None; Ryan Schmidt: None; Matthew Hiemenz: None; Gordana Raca: None; Robert Hutchison: None; Matthew Oberley: None

Background: Pediatric mature B-cell non-Hodgkin lymphoma (NHL) most commonly include Diffuse Large B-cell Lymphoma (DLBCL), Burkitt lymphoma (BL), and Primary Mediastinal B-cell lymphoma (PMLBCL).The pediatric MATCH trial enrolls children with specific genetic lesions that have matched therapies. On this trial, there are 9 target pathway alterations that have matched drugs: MTOR, MAPK, ALK, TRK, FGFR, EZH2, Cell Cycle, and/or BRAF V600E pathways. The frequency of alterations in these specific pathways in pediatric NHL is currently unknown.

Design: We identified patients diagnosed with NHL from the Children's Hospital Los Angeles (CHLA) pathology archive between 1991 and 2016. Clinicopathologic data was collected. Tissue Microarrays (TMA) were prepared from all cases of DLBCL, PMLBCL, and a subset of BL. IHC was performed to classify with 2016 WHO criteria. FISH for MYC and IRF4 was performed where appropriate. DNA and RNA were extracted from FFPE specimens for chromosomal microarray (CMA) (OncoScan, Affymetrix), and DNA and RNA sequencing (OncoKids, CHLA; RNAaccess, Illumina) on the Ion Torrent and Illumina platform respectively. Oncokids panel includes 40 of the 41 gene targets currently screened by the pediatric MATCH clinical trial.

Results: 60 cases of NHL were identified and characterized as BL (30 cases), DLBCL (17 cases), large B-cell lymphoma with IRF4 translocation (IRF4; 3 cases), or PMLBCL (10 cases). Clinicopathologic data of the cohort is presented in Table 1. Outcomes of lymphoma are worse in patients with concurring immunodeficiencies (logrank test P=0.006) (Figure1A). RNA sequencing from FFPE using the Burkitt molecular signature allowed for better diagnostic discrimination in borderline cases when considering DLBCL vs BL (Figure 1B). DNA sequencing identified targetable mutations in 44% (7/16) of cases tested so far, including PTEN, KRAS, BRAF, NF1, MAP2K1, EZH2, and CCND3. Recurrent chromosomal gains and losses were identified including those described previously in pediatric DLBCL cases (1q+, 6p LOH, 4p-, 11q+ and 19p-), and those described in both pediatric and adult DLBCL cases (2p+, 6q-, 12q+) Figure 2

Table 1. Clinicopathologic Data of the Cohort

Age/Sex	Location	Dx	Alive/ Dead	Immuno- deficiency	CD10	CD20	BCL6	MUM1	MYC	FISH MYC
13M	Peritoneum	DLBCL	Alive	No	0	100	80	50	40	3N
14M	Duodenum	DLBCL	Death	No	0	100	10	70	20	3-4N
14M	Lymph node	DLBCL	N/A	N/A	0	100	0	0	0	N/A
14M	Peritoneum	DLBCL	Alive	N/A	20	100	80	50	80	3N
15M	Lleocecum	DLBCL	Death	AT*	0	100	0	70	40	3-4N
17M	Lymph node	DLBCL	Alive	N/A	0	100	70	40	20	3-4N
1F	Paranasal sinus	DLBCL	N/A	N/A	0	100	30	50	0	N/A
5F	Lymph node	DLBCL	Death	No	0	100	40	60	20	3N
12M	Lymph node	DLBCL	Death	ADA-SCID*	80	100	90	0	20	2N
13F	Oropharynx	DLBCL	Death	AT	50	100	60	70	50	N/A
14F	Peritoneum	DLBCL	Alive	No	80	100	70	0	10	2N
17F	Peritoneum	DLBCL	Alive	No	80	100	50	0	10	2N
3M	Testicle	DLBCL	Alive	No	0	100	90	0	50	N/A
6M	Peritoneum	DLBCL	Alive	XLPS*	100	100	80	0	70	N/A
7M	Lymph node	DLBCL	Alive	No	100	100	80	10	0	3N
7M	Peritoneum	DLBCL	Alive	No	20	100	40	0	30	2N
9F	Pelvic mass	DLBCL	Death	No	100	100	90	0	70	>4N
14F	Larynx	IRF	Alive	No	100	100	70	90	50	2N
17M	Lymph node	IRF	Alive	No	0	100	90	90	50	N/A
7M	Tonsil	IRF	Alive	No	100	100	80	80	50	N/A
16F	Lymph node	PMLBCL	Alive	No	0	0	0	0	25	3N
18F	Lymph node	PMLBCL	Death	No	50	100	70	80	0	N/A
6F	Lung	PMLBCL	Death	AT *	0	100	10	100	60	3N
14F	Mediastinum	PMLBCL	Death	No	0	100	60	40	100	2N
15F	Mediastinum	PMLBCL	Death	N/A	0	100	50	80	0	N/A
15M	Mediastinum	PMLBCL	Death	N/A	0	100	30	50	10	N/A
16F	Mediastinum	PMLBCL	Alive	No	0	100	50	0	5	3N
16M	Mediastinum	PMLBCL	Alive	No	0	100	0	0	20	2N
17M	Mediastinum	PMLBCL	Alive	No	0	100	80	20	0	N/A
17M	Lymph node	PMLBCL	Alive	No	0	100	40	90	30	3N

*ADA-SCID = Adenosine deaminase deficiency-severe combined immunodeficiency, AT = Ataxia Telangiectasia, XLPS = X-linked lymphoproliferative syndrome

Figure 1 - 1774

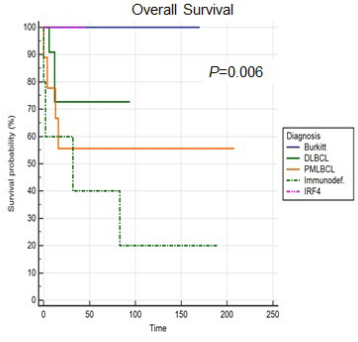

Figure 1A. Kaplan-Meier Curves for the different diagnostic cohorts for overall survival.

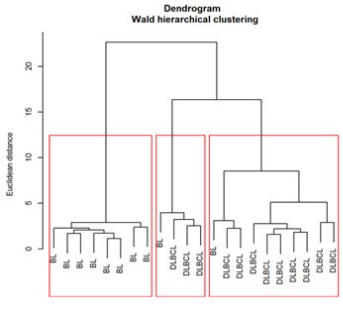

Figure 1B. Hierarchical clustering analysis of RNA sequencing data from DLBCL and Burkitt cases using a molecular Burkitt signature demonstrates that the DLBCL cohort is pure.

Figure 2 - 1774

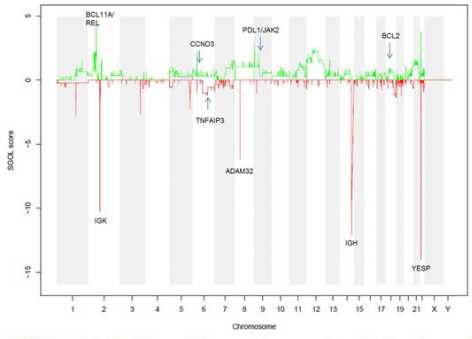

Figure 2. CMA analysis identifies multiple recurrent copy number alterations in our cohort. Green (gains) and Red (losses) are shown. Recurrent abnormalities include 1q+, 6p LOH, 4p-, 11q+, 19p-, 2p+, 6q-, 12q+.

Conclusions: Classification of pediatric NHL is facilitated by molecular analysis. Of 16 cases tested so far by sequencing, 7 have an identifiable mutation that would render them eligible for enrollment in the pediatric MATCH trial. Matching therapy to deregulated cellular pathways provides a much needed therapeutic option to patients with NHL who fail traditional chemotherapy.

1775 Cranial Fasciitis In Children: Clinicopathologic And Molecular Analysis of 11 Cases

Anas Bernieh[1], Youssef Al Hmada[1], Faizan Malik[2], Siraj El Jamal[3], Ali Saad[4]
[1]University of Mississippi Medical Center, Jackson, MS, [2]Memphis, TN, [3]Icahn School of Medicine at Mount Sinai, New York, NY, [4]Methodist/LeBonheur Health System, Memphis, TN

Disclosures: Anas Bernieh: None; Youssef Al Hmada: None; Faizan Malik: None; Siraj El Jamal: None; Ali Saad: None

Background: Cranial fasciitis (CF) is a rare benign soft tissue tumor of the scalp commonly encountered in children within the first 2 years of age. Similar to nodular fasciitis, it is hypothesized that a preceding trauma triggers reactive myofibroblastic proliferation. It is now established, however, that CF is a neoplastic process and nearly all cases harbor a *USP6* rearrangement. In this largest series to date, we report the clinicopathologic, immunoprofile, and molecular findings of 11 cases of CF in children.

Design: Pediatric patients with CF are collected from multiple institutions. Demographics and clinical follow-up are retrieved from the patients' medical records. A representative block from each case is immunostained for smooth muscle actin (SMA), beta-catenin, desmin, CD99, and S-100. Fluorescence in situ hybridization (FISH) for *USP6* rearrangement is performed on some of the cases.

Results: A total of 11 cases are collected. They consist of 5 males and 6 females. Median age is 2.3 years (range: 0.3-7 years) and the median size of the tumor is 3 cm (range: 1.2-10.6 cm). The tumor was solitary in 8 cases and multiple (2 lesions) in 3. In 9 cases, the family reported recent accelerated growth of the tumor which triggered medical attention. For the entire cohort, the tumor was reported to be present for a median time of 3.75 months (range 1-9 months). The tumor commonly involved the temporal area followed by the frontal. All cases were relatively poorly circumscribed. The tumor was limited to the soft tissue of the cranium in 6 cases, invaded the underlying bone in 3 cases and invaded the bone and dura in 2 cases. In all cases, the tumor was at least focally present at the surgical margin(s). Upon follow-up (median 7 months-range: 1-36 months), the tumor recurred in 4 cases a median of 10 months after surgery (range: 1-15 months).

In all cases, SMA showed patchy to diffuse positivity. Beta-catenin showed a cytoplasmic pattern of staining. S-100 showed rare positive cells and desmin and CD99 were negative. FISH for *USP6* rearrangement, available in 9 cases, was positive in 7 cases and negative in 2.

Conclusions: CF in children, now regarded a neoplastic process by virtue of harboring *USP6* rearrangement, is a benign process involving the soft tissue of the cranium. Owing to its infiltrative borders, complete excision is difficult to achieve. The tumor is commonly confined to the soft tissue but occasionally infiltrate adjacent structures. When confined to soft tissue, the tumor rarely recur but there is increased risk of recurrence when the tumor involves adjacent structures (bone and dura in our series). Apart from the positivity for SMA, immunohistochemistry is of little value and largely used to rule out other entities mimicking CF. In difficult cases, FISH to detect *USP6* rearrangement might be considered.

1776 Multifocal glomeruloid angiomatous malformations associated with lissencephaly II and POMT1 and JAM3 mutations

Victor Brochu[1], Moy-Fong Chen[1]
[1]McGill University Health Center, Montréal, QC

Disclosures: Victor Brochu: None

Background: Visceral angiomatous malformations have a complex differential diagnosis. We describe the autopsy findings of a male fetus terminated at 16+1 weeks gestation for suspected major brain anomaly, in which histology revealed incidental angiomatous malformations in bilateral lungs and thyroid, with a peculiar morphology not corresponding to any known specific entity. Additional findings revealed lissencephaly type II, a neuronal migration defect resulting from abnormal glycosylation of alpha-dystroglycan; and variants of unknown significance (VUS) in POMT1 (c.1483G>A, homozygous), a gene known for its interaction with alpha-dystroglycan, and JAM3 (c.-1C>T, heterozygous), a gene involved in cell-cell adhesion.

Design: Autopsy assessment and stains were performed according to the institution's clinical standards. Immunohistochemistry (IHC) was performed with a marker for vascular differentiation (CD31). Whole exome sequencing (WES) was performed on fetal cells culture from maternal blood.

Results: Histology revealed well-formed glomeruloid lesions, with single-feeding vessels from adjacent arterioles, found multifocally in the thyroid parenchyma and bilateral pulmonary septa at bronchovascular sites (Figure 1). IHC highlighted the feeding vessels and confirmed a vascular origin (Figure 2). The lesions were compared to an extensive differential diagnosis, including pulmonary vascular malformations, haemangiomas, and glomeruli forming neoplasms, with no single entity corresponding to the case's histology. Literature was reviewed for potential associations between visceral angiomatous malformations and lissencephaly, POMT1 and JAM3 alterations and their respective phenotypes, but yielded no contributory results.

Figure 1 - 1776

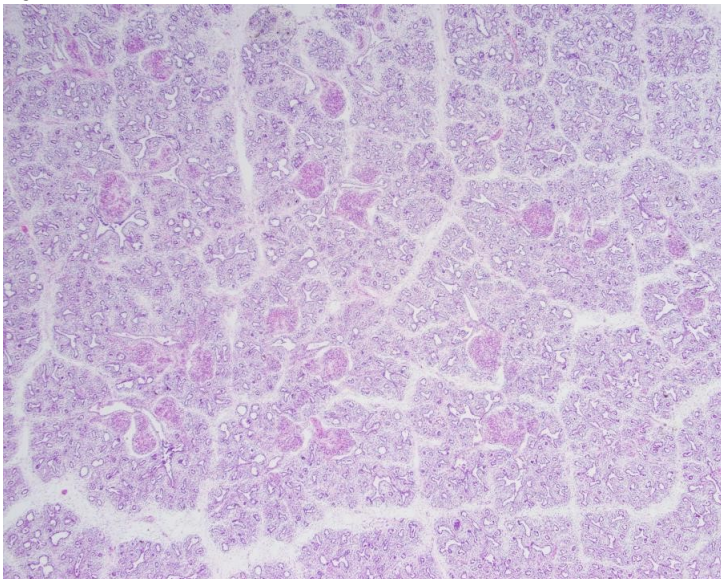

Figure 2 - 1776

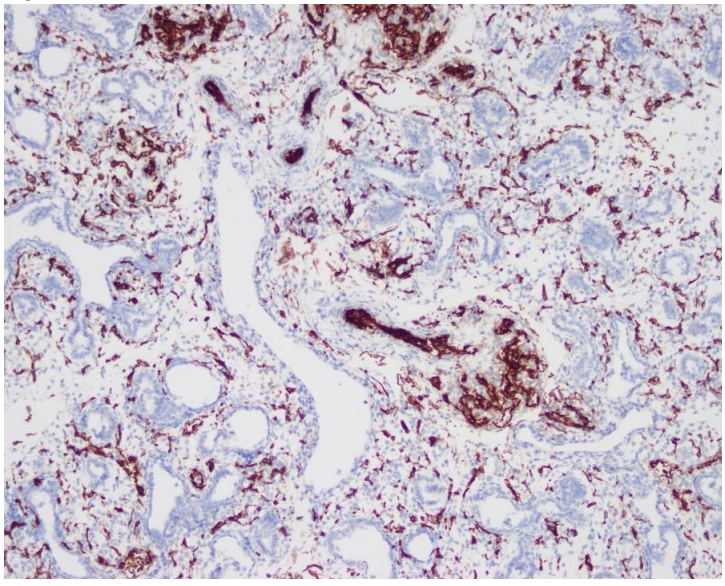

Conclusions: This case characterizes peculiar vascular lesions that, to the best of our knowledge, have not been previously described in the literature. This could raise the possibility of a new pathological entity. Coupled with the additional results, the case raises two hypotheses: the homozygous POMT1 VUS is speculated to be pathogenic, given the severity of the neuropathology findings and the known POMT1/lissencephaly association; and the constellation of genetic and phenotypic findings raises the possibility of a new association/syndrome. Future avenues include vast exposure to experts' opinion and potential molecular testing on the formalin-fixed, paraffin-embedded tissue.

1777 DNA Methylation Profiling in Pediatric Adrenocortical Tumors Reveals Distinct Methylation Signatures with Prognostic Significance: A Report from the International Pediatric Adrenocortical Tumor Registry

Michael Clay[1], Emilia Pinto[1], Cynthia Cline[1], Quynh Tran[1], Lin Tong[1], Elizabeth Azzato[1], Alberto Pappo[1], Michael Dyer[1], David Ellison[1], Stanley Pounds[1], Gerard Zambetti[1], Brent Orr[1], Raul Ribeiro[1]
[1]St. Jude Children's Research Hospital, Memphis, TN

Disclosures: Michael Clay: None; Emilia Pinto: None; Cynthia Cline: None; Quynh Tran: None; Lin Tong: None; Elizabeth Azzato: None; Alberto Pappo: None; Michael Dyer: None; David Ellison: None; Stanley Pounds: None; Gerard Zambetti: None; Brent Orr: None; Raul Ribeiro: None

Background: Pediatric adrenocortical tumors (ACTs) are rare neoplasms classified as adenoma, carcinoma (ACC), and tumor of uncertain malignant potential (UMP) based on a combination of histopathologic and clinical variables. Accurate diagnosis of ACTs is vital, especially as ACC is an aggressive neoplasm with a long-term clinical survival of 40-50%. The current classification scheme is hindered by poor reproducibility, and additional tools are needed to stratify patients into appropriate therapeutic risk categories.

Design: DNA methylation profiling (EPIC BeadChip Array), mutational assessment, immunohistochemistry (IHC), and comprehensive histopathologic analysis (Wieneke criteria) was performed on 52 pediatric ACTs with long term clinical follow-up. Cases represented the spectrum of neoplasia including adenoma (n=10), tumors of UMP (n=13), and ACC (n=29). Non-neoplastic adrenal tissue was included as a control (n = 13). Overall survival was used as a primary endpoint.

Results: Among the Wieneke histopathologic criteria, vascular invasion (HR=6.2, p=0.02), tumor weight (HR=10.9, p=0.001), and tumor size (HR=11.3, p=0.002) were significantly correlated with overall survival. Additional features including tumor volume (cm^3, HR=8.53, p=0.008), diffuse necrosis (HR=9.21, p=0.03), Ki-67 IHC (>40%, HR=7.1, p=0.02), patient age (>4 years, HR = 16.8, p=0.008), and clinical stage (HR = 9.8, p = 0.03) were also significant. Unsupervised analysis of the top differentially methylated probes segregated cases into two distinct groups (designated A1 and A2). The A1 subgroup had unique copy number changes and recurrent global hypomethylation of chromosomes 4, 13, and 18. Differentially methylated genes (q-value<0.05) between A1 and A2 groups included those associated with IGF-, mTOR, WNT, and HGF/cMET signaling pathways. Other genes commonly mutated in pediatric malignancies (*DICER1, EZH2, EGFR*, *PTEN*, *RB1, TERT, SF1, and MEN1)* were also differentially methylated. The A1 group was significantly associated with higher frequency of *CTNNB1* mutations (p = 0.03) and lower frequency of *TP53* mutations (p = 0.04). A combination of histopathology (diffuse necrosis, volume > 1000 cm^3), IHC (Ki67 > 40%), and methylation subgroup (A1) was strongly associated with survival (HR=24.5, p=1.7E-05).

Figure 1 - 1777

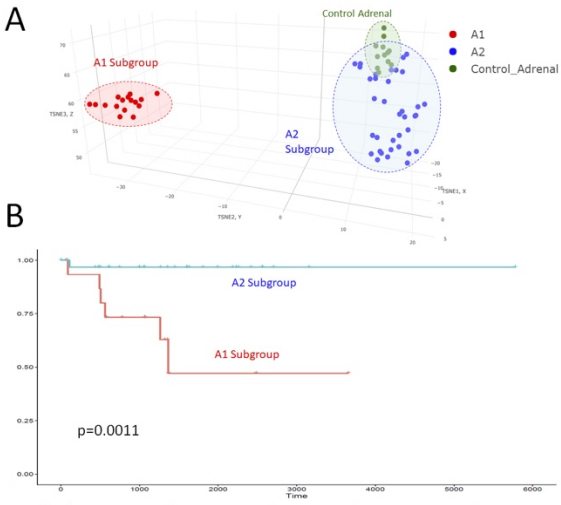

Methylation Profiling in Pediatric Adrenocortical Tumors
A) Unsupervised hierarchical clustering visualized with t-SNE shows two distinct subgroups of ACTs in addition to control adrenal tissue.
B) Kaplan-Meier highights decreased survival in the A1 sugroup.

Conclusions: Methylation profiling provides prognostic significance that is independent of pathologic diagnosis and stage, and in the future, may serve as a powerful biomarker in the prognostication of pediatric ACT.

1778 The Diagnosis of Pediatric Rhabdomyosarcoma is Improved by DNA Methylation Profiling: Identification of Distinct Molecular Subgroups Including Pure Spindled Rhabdomyosarcoma

Michael Clay[1], Anand Patel[1], Cynthia Cline[1], Quynh Tran[1], Sariah Allen[1], Lin Tong[1], Dale Hedges[1], Elizabeth Azzato[1], Stanley Pounds[1], Elizabeth Stewart[1], Alberto Pappo[1], David Ellison[1], Michael Dyer[1], Brent Orr[1]
[1]St. Jude Children's Research Hospital, Memphis, TN

Disclosures: Michael Clay: None; Anand Patel: None; Cynthia Cline: None; Quynh Tran: None; Sariah Allen: None; Lin Tong: None; Dale Hedges: None; Elizabeth Azzato: None; Stanley Pounds: None; Elizabeth Stewart: None; Alberto Pappo: None; David Ellison: None; Michael Dyer: None; Brent Orr: None

Background: Most pediatric rhabdomyosarcomas (RMS) can be separated histologically into embryonal (ERMS) or alveolar (ARMS) subtypes. Whereas ARMS are defined by recurrent *FOXO1* gene rearrangements, equivalent biomarkers for ERMS have not been well defined. Tumors with a spindle cell/sclerosing pattern (ssRMS), previously considered variants of ERMS, were recently separated in the 2013 revision of the WHO classification. These lesions are characterized by heterogeneous molecular features including *VGLL2* fusions, *NCOA2* fusions, and *MYOD1* mutations, and can be challenging to clinically classify.

Design: To determine whether DNA methylation profiling could be used as a biomarker to molecularly distinguish RMS groups, we performed Infinium EPIC BeadChip Arrays and histologic review on 149 RMS representing the spectrum of pediatric disease (ERMS=50, ARMS=54, ssRMS=4, Unclassified=41). To better understand the landscape of RMS, expanded analysis including RNA-seq was performed on cases with spindled morphology (sRMS).

Results: Unsupervised analysis of the top differentially methylated probes faithfully recapitulated clinical diagnoses with distinct grouping of ARMS and ERMS (100 of 104 cases). Classification was unaffected by therapy or metastasis when biological replicates from the same patient were available, and stable when evaluated in orthotopic patient-derived xenografts. Of the two discordant cases with sufficient materials, orthogonal testing supported the unsupervised model (overall 98% concordance). Of the 41 cases with uncertain initial diagnoses, 32 were reliably grouped by methylation profiling as either ERMS or ARMS. A separate cluster was formed by 9 remaining cases (7 unclassifiable, 2 ssRMS). This cluster, comprised of 3 males and 6 females aged 2 to 21 years (average 11 years), had uniform spindled morphology and a unique copy number profile when compared to the ERMS and ARMS cohorts. RNA-seq analysis identified a *MYOD1*mutation (c.365T>G; p.L122R) in every case, with concurrent *PIK3CA* variants identified in 2 of 9 cases. None harbored *FOXO1*, *NCOA2,* or *VGLL2* fusions. All patients for which clinical follow-up information was available were deceased (n=3).

Figure 1 - 1778

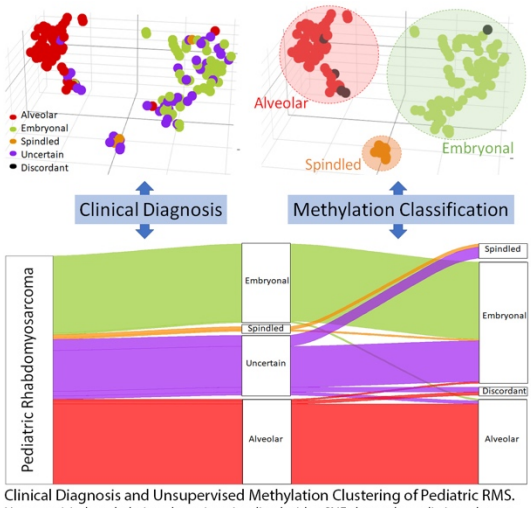

Clinical Diagnosis and Unsupervised Methylation Clustering of Pediatric RMS. Unsupervised methylation clustering visualized with t-SNE shows three distinct clusters (top left). Orthogonal validation (FISH/PCR) of methylation results shows high concordance with few discordant cases (black, top right). Alluvial plot (bottom) highlighting significant reclassification of initially uncertain diagnoses.

Conclusions: Taken together, our findings suggest methylation profiling provides a powerful biomarker for molecular classification of pediatric RMS. In addition to objective classification of 98% of samples (146/149), it effectively separated rhabdomyosarcomas with a spindled pattern (variant of ERMS, n=10) from true sRMS.

1779 Expression of Alpha-Synuclein in the Dysplastic Neurons of Pediatric Conventional Gangliogliomas; a Diagnostic Tool in Challenging Cases

Elizabeth Davaro[1], Alyssa Higgins[1], Miguel Guzman[1]
[1]Saint Louis University, St. Louis, MO

Disclosures: Elizabeth Davaro: None; Alyssa Higgins: None; Miguel Guzman: None

Background: Alpha-synuclein, (a-SYN) a pre-synaptic cytoplasmic protein found most abundantly in neural tissue, is widely known for its presence in neurodegenerative disorders. Gangliogliomas, benign tumors of the central nervous system (CNS) are characterized by dysplastic ganglion cells and neoplastic glial components, which have been described to exhibit neurodegenerative findings. The challenge in distinguishing conventional gangliogliomas from tumors with ganglioneuronal differentiation is highlighted by recent recategorization of classic gangliogliomas and pilocytic astrocytomas with gangliocytic differentiation. Distinctive immunostaining is therefore essential to their definitive identification. Wehypothesize that a-SYN expression can be used to highlight dysmorphic neurons present in conventional gangliogliomas and thus aid in the diagnosis of challenging cases.

Design: Immunohistochemistry for a-SYN was performed on a retrospective cohort of classic gangliogliomas (18) (study group) diagnosed at our institution, and were compared with 6 pilocytic astrocytomas, 1 dysembryoplastic neuroepithelial tumor (DNET), 1 atypical extraventricular neurocytoma, 1 subependymal giant cell neoplasm (SEGA), 1 case of cortical dysplasia, and 5 cases of reactive gliosis, which met inclusion criteria. Specimens were examined for eligibility, stained with human alpha-synuclein Ab-2 (clone syn211, 1/250, Thermo Scientific, MS-1572), and a blinded evaluation was performed independently by two reviewers. Cytoplasmic a-SYN staining in >5% of lesional cells was considered positive.

Results: Large, dysmorphic neurons showed cytoplasmic a-SYN immunoreactivity that met above criteria in 17 of 18 sampled conventional gangliogliomas. 1 of 1 SEGA was also positive. Cytoplasmic alpha-synuclein was negative in other neoplasms and processes. Pearson chi-square testing (performed with SPSS software program ver. 20.0) showed a statistically significant association between positivity of a-SYN immunohistochemistry and a diagnosis of classic ganglioglioma with a sensitivity of 94.4% and specificity of 93.3% (P-values <0.05 were considered statistically significant).

Figure 1 - 1779

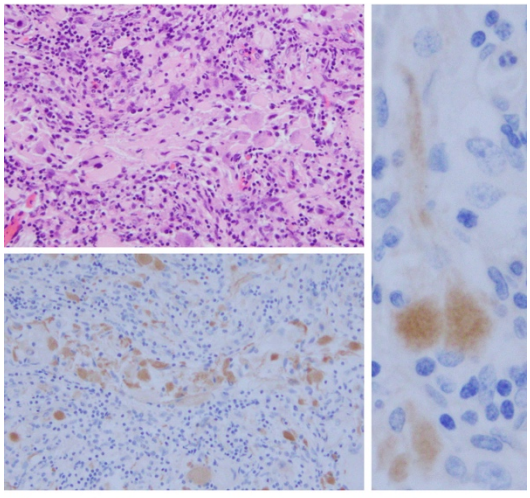

Figure 1: Classic ganglioglioma, H&E (A). α-Synuclein is expressed in the cytoplasm of dysmorphic neurons (B, C).

Figure 2 - 1779

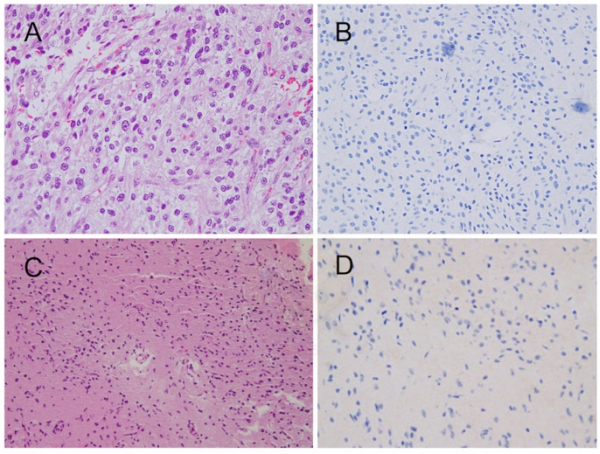

Figure 2: Low grade glioneuroal tumor (A, B), is completely negative for α-synuclein (B). α-Synuclein expression appears in only occasional neuritis in this case of pilocytic astrocytoma (C, D).

Conclusions: Cytoplasmic IHC labeling of neurons with alpha-synuclein is highly sensitive and specific for the diagnosis of ganglioglioma in the setting of pediatric CNS tumors. Our study provides evidence for the diagnostic utility of a-SYN's expression pattern in conventional gangliogliomas. We also aim to validate our findings in a cohort from another institution.

1780 Deep Juvenile Xanthogranuloma Harbors BRAF V600E Mutation Similar to Other Histiocytic Lesions

Julie Fanburg-Smith[1], Heidi Reinhard[2]
[1]Penn State Health Milton S. Hershey Medical Center, McLean, VA, [2]Penn State Health Milton S. Hershey Medical Center, Hershey, PA

Disclosures: Julie Fanburg-Smith: None; Heidi Reinhard: None

Background: Cutaneous juvenile xanthogranuloma (JXG) is considered a pediatric histiocytic tumor with eosinophils. We previously defined "deep" JXG (DJXG) to exclude cutaneous and extracutaneous visceral lesions and include only subcutaneous or intramuscular sites. BRAF mutation is present in other systemic, histiocytic disorders, including Langerhans and Erdheim-Chester.

Design: Cases coded as "intramuscular (IM)" or "subcutaneous (SQ)" JXG were included; dermal and other visceral JXG were excluded. Available clinicopathologic and radiologic data was reviewed. Immunohistochemistry and bi-directional squencing of exon 15 was performed to analyze BRAF mutation.

Results: There were 31 IM and 21 SQ DJXG in 30 males and 22 females; all but three were less than one-year of age. Sizes ranged 0.5-9.0 cm; IM were twice as large and more proximal than SQ. Locations included trunk (n=31), proximal extremity (n=13), and head-and-neck (n=6). One patient had a concurrent pituitary involvement with diabetes insipidus; the rest were solitary. DJXG had plump histiocytoid cells arranged in sheets, without atypia, and few normal-form mitoses; one case had focal necrosis. IM displayed infiltrative growth around skeletal muscle fibers and one case demonstrated smooth intraosseous scapular erosion. SQ were well-delineated, ball-like, across fascial planes. Overall eosinophils were minimal. Fibrosis and xanthoma cells were observed posttreatment in one patient. Immunostains: BRAF V600E+, CD14+, CD163+, CD68+, Factor XIIIa+, lysozyme+, CD10+, SMA+, focal rare nuclear CD30 and focal EMA, with mostly negative S100 protein, CD3, CD20, CD1a, CD21, CD35, CD34, ALK, EBER, desmin, and keratins. All cases studied harbored BRAF mutation V600E. Radiology excluded sclerotic symmetrical lesions of lower extremities or cardiopulmonary involvement. No patient died of disease, up to 29 years.

Conclusions: DJXG is a truncal pediatric histiocytic tumor with reversed infiltration of skeletal muscle to bone and nested subcutis pattern with relative eosinophil paucity. Deep proximal location, large size, mitoses, rare necrosis, and rare bone erosion can be worrisome in pediatric patients. CD1a, S100, and Langerin are negative, excluding Langerhans. BRAF V600E phenotype and mutation support a possible phenotypic relationship of DJXG to adult Erdheim-Chester, despite clinicoradiologic dissimilarity. A BRAF-inhibitor could be potentially useful in clinically challenging cases.

1781 Spectrum of Pediatric Cervical Pathology: the Dallas Experience

Melinda Flores[1], Amanda Strickland[1], Dinesh Rakheja[1]
[1]University of Texas Southwestern Medical Center, Dallas, TX

Disclosures: Melinda Flores: None; Amanda Strickland: None; Dinesh Rakheja: None

Background: Pediatric cervical pathology is largely understudied and although rare, can cause significant morbidity and potential mortality. We describe the spectrum and incidence of cervical pathology at our institution over the past 20 years.

Design: After approval by the Institutional Review Board, a review of all pathology reports from a large metropolitan pediatric hospital, from January 1, 1996 to April 1, 2017 was conducted. Inclusion criteria were specimens containing cervical tissue from female patients ranging from birth to age 21 years. Any cases from intersex patients, patients older than 21 years, or cases containing insufficient tissue for diagnosis were excluded.

Results: Cases were retrieved for 107 female patients who collectively underwent a total of 209 procedures yielding 287 diagnoses. The ages ranged from 3 years to 20 years (mean 15.9 years, median 16 years, mode 16 years). The most common procedures were cervical biopsy (n = 125, 59.8%), endocervical curettage (n = 76, 36.4%), and polypectomy (n = 3, 1.44%). The most common diagnostic category was infection (n = 138, 48.1%), of which condyloma acuminatum was the most common diagnosis (n = 99, 34.5% of all cases, 71.7% of diagnoses in the infectious category). The second most common diagnostic category was neoplasia (n = 75, 26.1%), which included CINI/LSIL (n= 51, 17.8% of all cases and 68% of all neoplastic cases), CIN II (n = 15, 5.23% of all cases, 20% of all neoplastic), CIN III (n = 5, 1.74% of all cases, 6.67% of all neoplastic cases), and leiomyosarcoma (n = 2, 0.697% of all cases, 2.67% of all neoplastic cases). No histopathologic abnormality was identified in 73 (25.4%) cases. Over half of all cases (n = 170, 59.2%) were related to the human papillomavirus (HPV).

Conclusions: This is one of the largest clinico-pathologic studies of pediatric cervical lesions. The majority of the diagnoses relates to HPV infection, and reflects the cervical cancer screening guidelines at the time. Notably, the significant number of cases deemed to have no histopathologic abnormality was expected as many of the endocervical curettages yielded no HPV involvement. As HPV vaccination becomes more widespread, the number of HPV related cases is expected to decrease. Similar studies from around the world may illustrate any geographic or ethnic variations in pediatric cervical pathology.

1782 Evaluating and Defining Follicular Hyperplasia in the Appendixes of Children with Chronic Right Lower Quadrant Abdominal Pain

Catherine Forse[1], Sarah Worley[1], Jessica Barry[2], Lori Mahajan[1], Federico Seifarth[3], Thomas Plesec[1]
[1]Cleveland Clinic, Cleveland, OH, [2]Cleveland, OH, [3]Kalispell Regional Healthcare, Kalispell, MT

Disclosures: Catherine Forse: None; Thomas Plesec: None

Background: Studies suggest that appendectomy can improve chronic abdominal pain in children despite the absence of histological features of acute/ interval appendicitis. The purpose of this study was to compare the appendixes from children who responded to appendectomy for chronic pain to age-matched controls in order to identify defining histological features. In particular, this study focused on evaluating appendiceal lymphoid hyperplasia as there is no specific definition in the literature.

Design: The appendixes of 30 children who had chronic pain and were symptom-free post-surgery were compared to those of 16 children who did not have chronic pain or appendicitis. The degree of lymphoid hyperplasia was determined by measuring the number of germinal centers (GCs) per 5 mm and the greatest diameter of 5 consecutive GCs using an ocular ruler. Appendixes were only included if they had a complete cross-section of the appendix tip. Study groups were compared on GC size using the two sample t-test, and on GC adjusting for age using two-methods: 1) paired t-test on subjects matched by age, and 2) ANCOVA regression model for GC by group, age, and group-age interaction. All analyses were performed on a complete-case basis. All tests were two-tailed and performed at a significance level of 0.05. SAS 9.4 software (SAS Institute, Cary, NC) was used for all analyses. The performance of counting the number of GCs/ 5 mm for identifying lymphoid hyperplasia was evaluated by calculating the sensitivity (Sn), specificity (Sp), positive predictive value (PPV) and negative predictive value (NPV).

Results: Qualitatively, there were no differences observed in inflammation or fibrosis between the two cohorts. Children with chronic pain had significantly more GCs/ 5 mm than age-matched controls (mean difference: 3.3, P<0.001(95% CI)). There was no significant difference in the average size of individual GCs. Using a cutoff of ≥ 9 GCs/5 mm as an assessment for follicular hyperplasia had a Sn of 80%, Sp of 73.3%, PPV of 85.7% and NPV of 64.7%.

Conclusions: Follicular hyperplasia as defined by ≥9 GCs/ 5 mm is significantly associated with resolution of chronic abdominal pain post-appendectomy. Pathologists should be aware of this feature when assessing the appendix of children with chronic abdominal pain.

1783 Neuropeptide "Y" Triggers Perineural Invasion in Ewing Sarcoma via Y1 Receptor Expressed in Tumor Cells

Susana Galli[1], Sara Misiukiewicz[2], Sung-Hyeok Hong[3], Shiya Zhu[4], Kitlinska's Lab[4], Nouran Abualsaud[5], Lucia Gempel[6], Jason Tilan[3], Joanna Kitlinska[3]
[1]Rockville, MD, [2]Washington, DC, [3]Georgetown University Medical Center, Washington, DC, [4]Georgetown University, Washington, DC, [5]Georgetown University Medical Center, Arlington, VA, [6]Georgetown University Medical Center, Rockville, MD

Disclosures: Susana Galli: None; Sara Misiukiewicz: None; Sung-Hyeok Hong: None; Shiya Zhu: None; Kitlinska's Lab: None; Nouran Abualsaud: None; Lucia Gempel: None; Joanna Kitlinska: None

Background: Neuropeptide Y (NPY) is released from peripheral sympathetic nerves, but also highly expressed in Ewing Sarcoma (ES) along with its Y1, Y2 and Y5 receptors. Our previous data indicated that in ES xenografts with low endogenous NPY expression, the peptide released from the neighboring peripheral nerves becomes a chemoattractant for the tumor cells rich in its receptors. This, in turn, stimulates profound perineural invasion (PNI) in these tumors. In contrast, in ES xenografts that release its own NPY, the endogenous peptide saturates its receptors and attenuates chemotactic effect of the neuronal peptide.

Design: The goal of this study was to identify NPY receptors mediating this effect. To this end, we tested three ES cells lines (TC-32, TC-71 and SK-ES1) varying in their endogenous NPY levels in an orthotopic xenograft model. ES cells were injected into the gastrocnemious muscles of the SCID/beige mice. After reaching the desired volume, the primary tumors were excised by limb amputation and subsequent metastasis monitored by MRI and confirmed by histopathological analyses. Expression of NPY receptors and neuronal markers was assessed by immunohistochemistry (IHC). *In vitro* Transwell migration assay was performed to test chemotactic effect of NPY in ES cells, in the presence or absence of selective antagonists targeting its receptors.

Results: The xenografts derived from ES cells with low endogenous NPY (TC71, TC32) exhibited frequent PNI in primary tumors, as well as recurrent tumors and metastatic paravertebral tumors. These processes were less common in ES xenografts derived from NPY-rich SK-ES1 cells. The metastatic paravertebral tumors accumulated around NPY-positive sympathetic and dorsal root ganglia, as determined by IHC for tyrosine hydroxylase and NeuN, respectively. All tumors expressed high levels of Y1, Y2 and Y5 NPY receptors. However, an *in vitro* migration assay identified NPY/Y1 axis as the main stimulator of PNI. Y1R antagonist blocked migration of ES cells toward NPY. Moreover, the chemotactic effect of NPY was significantly elevated in TC32 and TC71 cells with low endogenous NPY, but higher Y1R expression, as compared to NPY-rich SK-ES1 cells with low Y1R.

Conclusions: Altogether, our data indicate that Y1R plays an important role in the chemotactic properties of NPY and may trigger PNI in ES. If the presence of perineural tumor growth is confirmed in human ES, Y1 receptor may become a target for novel therapies preventing disease dissemination and recurrence.

1784 Pediatric Adrenocortical Tumors. Which Pathological Criteria System is the Best?

M. Laura Galluzzo Mutti[1], Maria Celeste Mattone[1], Alejandra Casanovas[1], Ezequiel Nespoli[1], Alicia Belgorosky[1], Gabriela Guercio[1], Fabiana Lubieniecki[2]
[1]Hospital Garrahan, Buenos Aires, Argentina, [2]Hospital de Pediatria J.P.Garrahan, Buenos Aires, Argentina

Disclosures: M. Laura Galluzzo Mutti: None; Maria Celeste Mattone: None; Alejandra Casanovas: None; Ezequiel Nespoli: None; Alicia Belgorosky: None; Gabriela Guercio: None; Fabiana Lubieniecki: None

Background: Adrenocortical Tumors (ACT) are rare in the pediatric group. The aim of this study was to evaluate different criteria systems in pediatric ACT, and correlate them with clinical outcome.

Design: We reviewed 24 cases of pediatric ACT, treated in our institution between 1987-2017. Weiss, modified Weiss and Wienecke criteria were applied, P53 and Ki 67 immunostaining were performed. Tumor weight, clinical data, staging (COG system), and therapeutic interventions were also evaluated.

Results: Mean age at diagnosis was 4.6 years (range 0.3-17.3), and female/male ratio was 2.5/1. Mean duration of symptoms was 10.9 months. Initial clinical signs were hormonal overproduction (virilization, Cushing's syndrome) in 57.1%, abdominal mass/pain in 35.7%, and hypertensive encephalopathy in 7.1. Disease free survival and overall survival was 100% for stage I and II, and 51% and 33% for stage III and IV respectively (eight patients received adjuvant chemotherapy with cisplatin, etoposide and doxorubicin). Tumor staging correlated positively and significative with tumor weight and with Wieneke criteria ($p<0.01$) as well. Median follow-up was of 3.64 years (range 0-12).

Weiss	Modified Weiss	Wienecke	Ki67	p53	weight	stage
3	1	1	low	1	22	1
7	5	3	low	1	60	1
6	3	2	low	0	9	1
8	7	3	low	1	40	1
0	0	0	low	0	42	1
6	4	3	high	1	25,88	1
8	7	4	low	1	162	2
3	4	4	low	1	620	2
9	7	4	low	1	204	2
6	4	4	low	1	283,3	2
9	7	4	low	1	145	2
8	5	4	high	1	355	2
8	7	6	high	1	77,2	3
9	7	6	low	1	570	3
6	3	4	low	1	283	3
4	5	3	low	0	420	3
6	4	4	low	1	5,5	3
9	7	7	high	1	348	3
6	4	4	low	0	93,2	3
7	4	4	low	0	202	3
9	7	8	high	1	1420	3
8	6	3	low	1	178	4
9	7	8	high	1	2460	4
9	7	5	high	0	325	4

Conclusions: Pediatric ACT tumors are rare (24 cases in 30 years in a large pediatric hospital) with hormonal hyperproduction being the most common clinical sign. In our cohort, comparative systems showed that only Wienecke criteria correlated with tumor weight and tumor staging. Stages I and II have the best patient outcome.

1785 Wilms Tumor with Renal Cell Carcinoma - A Rare Combination

Nilda Gonzalez Roibon[1], M. Laura Galluzzo Mutti[1], Ezequiel Nespoli[1], Fabiana Lubieniecki[2]
[1]Hospital Garrahan, Buenos Aires, Argentina, [2]Hospital de Pediatria J.P.Garrahan, Buenos Aires, Argentina

Disclosures: Nilda Gonzalez Roibon: None; M. Laura Galluzzo Mutti: None; Ezequiel Nespoli: None; Fabiana Lubieniecki: None

Background: Wilms tumor (WT) is the most common pediatric renal tumor, and renal cell carcinomas (RCC) account for about 2 % of tumor in the pediatric age. RCC has only rarely been reported to occur in association with WT. This study describes clinico-pathologic characteristics of 3 cases of WT with areas of renal cell carcinoma

Design: We performed a retrospective search from 2001-2018 in the surgical pathology files of our institution for WT showing areas of RCC. Whole sections from formalin-fixed-paraffin-embedded tissue were assessed for confirmation of diagnosis. Appropriate immunohistochemistry (IHC) was performed. Diagnosis, staging and treatment were assigned under SIOP 2001 protocol.

Results: We identified areas of RCC in 3/144 WT . Two patients were female, age at diagnosis ranged from 3 to 5 years. Cases 1 and 2 were stage 3 at diagnosis (positive regional lymph nodes), case 3 was stage 1. WT were epithelial-type, mixed-type and diffuse anaplasia (1 case each). RCC areas in primary tumors were intermixed with WT. Case 1: edematous papillae with occasional foamy histiocytes lined by cuboidal cells with scant cytoplasm and round nuclei (papillary RCC type1). Lymph nodes metastasis was given only by epithelial component with these features. In case 2 the RCC component was evident in the specimens from relapse (lung and abdominal lymph node), showing papillary RCC features as the predominant component. Immunostains were focally positive for CD56, WT1 and CK7 in both. Case 3 showed tubules lined by plump cells with abundant eosinophilic dense cytoplasm and vesicular nuclei with irregular contours. These areas were focally positive for CD10 and WT1 (unclassified RCC type). Patients received treatment following SIOP 2001 protocol for WT. Cases 1 and 3 are alive with 1 month of follow up. Case 2 showed no response to different lines of WT treatment.

Conclusions: WT may show very different features in the three classic components, but RCC areas are not part of them. Given their rarity, WT with RCC areas are not considered in the WHO classification (2016) or in different international protocols. In our series two cases showed a major component of RCC at the metastatic sites; one of them was present at diagnosis and the other in the progression of the disease. The latter was resistant to conventional WT treatment. It is a matter to consider if these children could benefit from a different type of treatment, especially when RCC is the predominant component.

1786 Expanding the Phenotypic Spectrum of the Extrapulmonary Manifestations of Alveolar Capillary Dysplasia with Misalignment of Pulmonary Veins; a 17-Year Case Series

Matthew Hedberg[1], Louis Dehner[1]
[1]*Washington University School of Medicine, St. Louis, MO*

Disclosures: Matthew Hedberg: None; Louis Dehner: None

Background: Since its formal description in 1981, ≈200 cases of alveolar capillary dysplasia with misalignment of the pulmonary veins (ACD/MPV), a lethal developmental lung disorder, have been reported. ACD/MPV classically presents with respiratory distress and cyanosis secondary to severe pulmonary hypertension and insufficient gas exchange during the first 24 hours of life; and is diagnosed by biopsy. Haploinsufficiency of *FOXF1* has been established as causative in ACD/MPV, though the full spectrum of genetic and developmental phenotypes remains unknown, and a number of extrapulmonary abnormalities continue to be described. We present a series of 5 autopsies from 3 male and 2 female ACD/MPV patients, who survived from 4 hours to 18 months, featuring several congenital abnormalities not previously associated with ACD/MPV, and one of the first ACD/MPV patients to receive a bilateral lung transplant.

Design: Electronic autopsy records at Barnes Jewish Hospital in St. Louis were queried for cases of ACD/MPV. Autopsy reports and medical records were reviewed and compiled; along with available genetic reports, gross examination images and photomicrographs to yield a comprehensive characterization of the spectrum of ACD/MPV phenotypes seen in our single center experience.

Results: In this autopsy series of patients with histopathologically confirmed ACD/MPV, we identify a number of congenital abnormalities not previously reported, to our knowledge, in association with ACD/MPV (see Table 1). These include gastric hamartomas, cavum septum pellucidum, cerebellar heterotaxy of Brun and uterus didelphys. In the most recent case of this series, autopsy revealed severe laryngeal stenosis which compromised intubation and was a contributing cause of death. We identified only one other case report from Japan with this finding. Which may become increasingly important as several institutions are now attempting lung transplants in ACD/MPV patients who must receive sufficient cardiopulmonary stabilization while awaiting surgery.

Case	Age	Sex	Surgical Interventions	Genetics	Gross/Congenital Abnormalities
1	4 hours	F	Bilateral chest tubes	16q24.1 deletion (1.66Mb)	Severe subglottic laryngeal stenosis with associated pulmonary hyperplasia R>L, bilateral bilobed lungs, ASD, gallbladder agenesis, bilateral renal dysplasia with left sided hypoplasia and right-sided hydronephrosis secondary to distal right ureteral stenosis/atresia, didelphic uterus, small for gesational age placenta with retroplacental hematoma and two-vessel umbilical cord
2	18 months	F	ECMO and bilateral lung transplant	Unknown	Cardiac abnormalities consistent with PHTN
3	11 weeks	M	ECMO	Unknown, but familial history of ACD/MPV	Pulmonary hypoplasia, cardiac abnormalities consistent with PHTN and surgical intervention, gastric hamartomas, intestinal malrotation, cavum septum pellucidum
4	8 days	M	Left chest tube	Chromosomal analysis showed trisomy 21	Bilateral pulmonary hyperplasia, oblique palpebral fissures, left transverse palmar crease, hepatomegaly, bilateral undescended testes, macroscopic brain appearance consistent with trisomy 21 demonstrating cerebellar hypoplasia with heterotaxia
5	2 weeks	M	ECMO	Unknown	Pulmonary hyperplasia, patent membranous foramen ovale, hepatomegaly, thymic hypoplasia, Hirschsprung disease

Conclusions: This case series expands the phenotypic spectrum of congenital abnormalities known to occur in the setting of ACD/MPV and highlights the markedly wide range of presentations. From cases with severe developmental abnormalities across multiple organ systems, to a case that presented with almost no extrapulmonary manifestations and was successfully treated, for a time, with a bilateral lung transplant. Until the patient succumbed to rejection and overwhelming chronic pulmonary infec

1787 Immunohistochemical Evidence of Hypoxia in Placentas with Preeclampsia and Chorangiosis

Amandeep Kaur[1], Linda Ernst[1]
[1]University of Chicago at NorthShore HealthSystem, Evanston, IL

Disclosures: Amandeep Kaur: None; Linda Ernst: None

Background: Carbonic anhydrase IX (CAIX) is an enzyme which catalyzes the conversion of carbon dioxide and water to bicarbonate and hydrogen ions. It has been shown to be induced in hypoxic states and is regulated by the induction of the transcriptional complex hypoxia-inducible factor-1 (HIF-1). Due to its association with hypoxia, immunohistochemical expression of CAIX has been extensively studied in a variety of tumor types, however there is a paucity of literature describing its expression in non-neoplastic tissues like placenta. Chronic hypoxia is thought to underlie placental pathologic conditions including preeclampsia, which is characterized by maternal vascular malperfusion (MVM) and chorangiosis, which is characterized by villous hypercapillarization. Therefore, our aim is to examine the expression of CAIX in placentas with clinically diagnosed preeclampsia and compare them to chorangiosis and controls using immunohistochemistry.

Design: Placental tissue was collected from January 1, 2017 to July 1, 2018 in 10 women with a clinical diagnosis of preeclampsia and MVM histology, 10 women with chorangiosis and 9 control placental tissues with no histopathologic abnormalities and immunohistochemistry for CAIX performed on parenchymal sections containing basal plate. A semi quantitative scoring system was used for strong membranous CAIX staining where a 1+, 2+ and 3+ score was given to <10%, 11-19% and >19% respectively.

Results: Some CAIX staining was present in all cases, but the strongest membranous staining was seen on the basal plate in extravillous trophoblasts (EVT) cells. CAIX expression in EVT was more prevalent in cases with MVM than either controls or chorangiosis. 40% of MVM cases had prominent membranous (3+) staining of EVT in basal plate vs 0% of controls and 10% of chorangiosis cases. When grouped as a dichotomous variable with <20% staining (1+, 2+) vs 20% or more (3+), the correlation approached statistical significance (p=0.053). All cases showed variable CAIX cytoplasmic blush in EVT but cytoplasmic staining of villous trophoblasts was seen in fewer cases (n=9) including 40% of MVM, 44.4% of controls and 10% of chorangiosis.

Conclusions: There is a marginal statistically significant increase in CAIX staining of EVT in MVM cases vs controls and no difference in CAIX staining in chorangiosis cases vs controls. This suggests that HIF-1 pathway is activated in MVM at the basal plate, but not as strongly in chorangiosis.

1788 Low-grade Osteosarcomatous Transformation of Atypical Lipomatous Tumor in a Pediatric Patient

Benjamin Kukull[1], Jessica Davis[1], Mazdak Khalighi[1], Christopher Corless[2], Barry Hansford[1], Kenneth Gundle[1]
[1]Oregon Health & Science University, Portland, OR, [2]Portland, OR

Disclosures: Benjamin Kukull: None; Jessica Davis: None; Mazdak Khalighi: None; Christopher Corless: None; Barry Hansford: None; Kenneth Gundle: None

Background: Atypical lipomatous tumors (ALT) are well-differentiated (WD) mesenchymal neoplasms, genetically driven by amplification of chromosome 12q (including amplification of genes MDM2 and CDK4). These tumors are exceptionally rare in the pediatric population and, when occurring in this setting, are strongly associated with Li-Fraumeni syndrome. Low-grade (LG) osteosarcomas (i.e. parosteal and LG central osteosarcoma) share the same genetic driver with amplification of MDM2/CDK4 and are also rare in children.

Design: We present an adolescent girl with an ALT and subsequent development of a LG osteosarcomatous proliferation favored to represent transformation of her ALT, with genetic confirmation.

Results: The patient presented at 13 years with a slow-growing 10.5-cm soft tissue mass centered within her left gastrocnemius muscle. The tumor was excised and showed a WD adipocytic neoplasm with broad fibrous bands, atypical hyperchromatic cells, and areas of myxoid change, which extended to the margins. Florescence in situ hybridization (FISH) showed MDM2 amplification, confirming the diagnosis of ALT.

The patient re-presented at age 15 with a 4.1-cm lesion on the surface of her posterior tibia, adjacent to the site of prior ALT. Imaging showed an osteoid-forming surface lesion without intralesional fat. Subsequent biopsy demonstrated an atypical fibro-osseous proliferation with parallel to anastomosing bony trabeculae and intervening mildly atypical spindle cells within a fibrous matrix. The spindle cells expressed MDM2 by IHC and showed MDM2 amplification by FISH. The differential diagnosis included parosteal osteosarcoma and LG osteosarcomatous transformation of the patient's ALT. Subsequent resection showed a minute focus of lipomatous and myxoid tissue adjacent to the osteosarcomatous component, likely representing residual/recurrent ALT or a shared, ill-defined neoplastic progenitor. Massive parallel sequencing (124 gene panel) of both elements confirmed MDM2 amplification but showed no other alterations (including TP53).

Conclusions: Rare cases of LG osteosarcomatous differentiation in WD liposarcoma have been described, but, to our knowledge, not in an ALT or in a pediatric patient. This case highlights a possible link between these two morphologically distinct, but genetically-identical neoplasms, and raises the possibility of distinctive biological behavior and clinical course for "adult" tumors occurring within the pediatric population.

1789 Histological Severity Risk Factors Identification in Juvenile-Onset Recurrent Respiratory Papillomatosis: About a 48 Patients Cohort

Charles Lépine[1], Louise Galmiche[2], Thibault Voron[3], Hélène Péré[1], Marion Mandavit[3], Eric Tartour[1], Sophie Outh-Gauer[1], Dominique Berrebi[4], Nicolas Leboulanger[5], Cecile Badoual[6]
[1]Hôpital Européen Georges Pompidou, APHP, Paris, France, [2]Paris, France, [3]Inserm U970, Paris, France, [4]Hôpital Robert Debré, APHP, Paris, France, [5]Hôpital Necker-Enfants Malades, APHP, Paris, France, [6]G Pompidou Hospital, Paris, France

Disclosures: Charles Lépine: None; Louise Galmiche: None; Thibault Voron: None; Hélène Péré: None; Marion Mandavit: None; Eric Tartour: None; Sophie Outh-Gauer: None; Dominique Berrebi: None; Nicolas Leboulanger: None; Cecile Badoual: None

Background: Juvenile-onset recurrent respiratory papillomatosis (JoRRP) is a condition characterized by the repeated growth of benign exophytic papilloma in the respiratory tract. JoRRP is caused by an HPV infection, usually by 6 and 11 genotypes. The course of the disease is still unpredictable: some children experience minor symptoms with spontaneous remission, while others require multiple interventions due to florid growth. Uncommonly the disease may transform into malignant lesions. Our study aimed to identify severity risk factors in the JoRRP.

Design: Forty-eight children were included retrospectively from two French pediatric centers. The criteria for a severe disease were: an annual rate of surgical endoscopy ? 5, a spread to the lung, a carcinomatous transformation or the death. Immunohistochemistry and chromogenic *in situ* hybridization (CISH) were performed on sections of FFPE tissue samples of laryngeal papilloma obtained between 2008 and 2018. We conducted immunostaining against p16, p53 and p63 combined with a CISH against E6 and E7 mRNA transcripts of HPV 6 and 11. Immunostainings against p63 and p53 were analyzed with an artificial intelligence-based software allowing semi-quantitative measures (number of nuclei exhibiting weak, medium and strong staining, as shown in the figure). CISH staining strength was divided in two categories: 1+ (weak) and 2+ (strong).

Results: A total of 24 patients had a severe disease, which was associated with a higher percentage of nuclei stained by both p63 and p53 antibodies, as shown in the table. For medium and strong straining combined together, a p53 antibody staining rate ? 4,5% and a p63 antibody staining rate ? 30% were associated with severity (p=0,001). Score 2+ in CISH tended to be associated with severity (p=0,067). All p16 immunostainings were negative. Compared to patients with a 1+ score in CISH, patients with a 2+ score had a higher frequency of surgical endoscopy during the first year (2 versus 5; p=0,029) and a higher annual rate (2,8 versus 6,1; p=0,036).

	Intensity of the staining	Mild disease (24)	Severe disease (24)	p
% of nuclei stained by antibody against p53 (median)	**Weak**	57,76	57,92	0,523
	Medium	3	4,46	**0,037**
	Strong	0,07	0,14	**0,011**
	All of the 3	62,1	65,22	0,216
	Weak and medium combined	3,22	4,57	**0,019**
% of nuclei stained by antibody against p63 (median)	**+**	55,7	49,56	0,095
	++	23,99	36,1	**0,043**
	+++	0,16	0,74	0,138
	All of the 3	82,19	86,07	0,127
	Weak and medium combined	24,1	36,9	**0,043**

Figure 1 - 1789

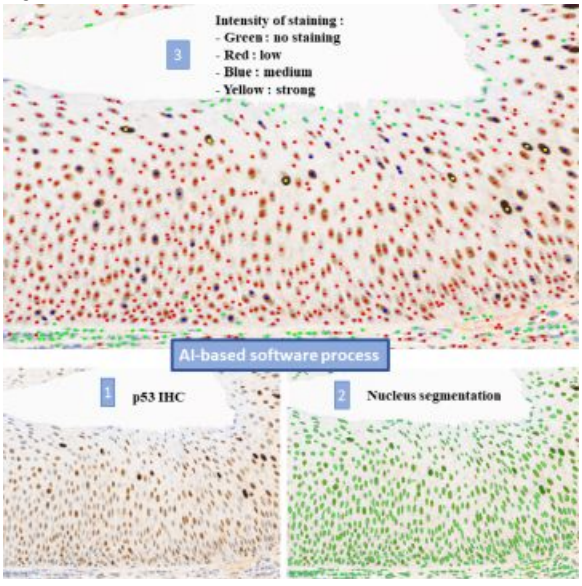

Conclusions: In conclusion, we pointed out using computerized image analysis, that our p53/p63 immunostaining signature is associated with severity in JoRRP. E6 and E7 mRNA CISH, that reflects the viral transcriptional activity of HPV, may be a promising severity risk factor to be explored in further larger cohorts.

1790 Correlation of BCOR Internal Tandem Duplication with NGFR, BCOR and Cyclin D1 Immunohistochemical Expression in Clear Cell Sarcoma of the Kidney

Kara Lombardo[1], Angshumoy Roy[2], Nick Shillingford[3], Fu-Yuan Shih[4], Sonja Chen[5], Evgeny Yakirevich[5], Shaolei Lu[6], Andres Matoso[1], Shamlal Mangray[7], Miriam Conces[8]
[1]Johns Hopkins Medical Institutions, Baltimore, MD, [2]Houston, TX, [3]Children's Hospital Los Angeles, Los Angeles, CA, [4]Texas Children's Hospital and Baylor College of Medicine, Houston, TX, [5]Rhode Island Hospital, Providence, RI,[6]Providence, RI, [7]Nationwide Children's Hospital, Providence, RI, [8]Nationwide Children's Hospital, Columbus, OH

Disclosures: Kara Lombardo: None; Angshumoy Roy: None; Nick Shillingford: None; Fu-Yuan Shih: None; Sonja Chen: None; Evgeny Yakirevich: None; Shaolei Lu: None; Andres Matoso: None; Shamlal Mangray: None; Miriam Conces: None

Background: Distinguishing clear cell sarcoma of the kidney (CCSK) from other renal neoplasms remains a challenge. Molecular alterations such as *BCOR* internal tandem duplication (ITD) in a majority of CCSKs, as well as a *YWHAE-NUTM2B* in a smaller subset of cases, have been reported, but available molecular testing in clinically validated labs is limited and expensive. Immunohistochemistry (IHC) for BCOR and cyclin D1 have been shown to correlate with these alterations, respectively, though neither is entirely specific. A recent study has reported that IHC for nerve growth factor receptor (NGFR) is a sensitive marker for CCSK. We sought to characterize the *BCOR* ITD status of a series of CCSKs and compare expression of NGFR, BCOR and cyclin D1 with other renal neoplasms.

Design: Molecular testing for *BCOR* ITD was performed by PCR and Sanger sequencing on eleven archival cases of CCSKs. IHC for NGFR, BCOR, and cyclin D1 was performed on tissue sections. Intensity (0=absent, 1+=weak, 2+=moderate and 3+=strong) and extent (< 10%, 10-50% and >50%) of nuclear staining for BCOR and cyclin D1 and membranous staining for NGFR were scored. Cytoplasmic NGFR staining was considered negative. IHC expression in CCSKs was compared to the blastemal components of 10 Wilms tumors (bWTs), 4 mesoblastic nephromas (MNs; 2 cellular, 2 classic), 3 infantile fibrosarcomas (IFs), 5 primary renal *CIC*-rearranged sarcomas, 1 renal EWS and 1 malignant rhabdoid tumor (MRT).

Results: Ten of 11 (91%) of CCSKs were positive for *BCOR* ITD (Table). All cases of CCSKs demonstrated diffuse (>75% of cells), 2+ to 3+ membranous staining with NGFR and nuclear staining with the BCOR and cyclin D1 antibodies (100% sensitivity). None of the other tumors were positive with NGFR. Focal (20%) 2+ BCOR IHC staining was seen in 1/10 bWTs, diffuse 2+ to 3+ cyclin D1 staining was seen in 1/3 IFs and the renal EWS. Cyclin D1 was focally expressed in 7/10 bWTs, 2/3 IFs, 2/2 cellular MNs, and 2/2 classic MNs with 2+ to 3+ staining. All other tumors were negative. The specificity, PPV and NPV for NGFR was 100% in the cases studied compared to 95.8%, 91.7% and 95.8% for BCOR, and 35.7%, 42.3% and 37.5% for cyclin D1 respectively.

Table. Correlation of *BCOR* ITD status and immunohistochemical expression in CCSKs

Case No.	Age (y) & Gender	*BCOR*ITD Status	NGFR	BCOR	Cyclin D1
1	19/M	Negative	90% 3+	90% 3+	90% 3+
2	6/M	Positive	90% 3+	90% 3+	90% 3+
3	1/M	Positive	50% 3+	90% 3+	90% 3+
4	3/F	Positive	75% 3+	90% 3+	90% 3+
5	2/M	Positive	75% 2+	90% 3+	90% 3+
6	17/F	Positive	75% 3+	90% 3+	90% 3+
7	1/F	Positive	75% 3+	90% 3+	90% 3+
8	2/M	Positive	90% 2+	90% 2+	75% 2+
9	4/M	Positive	90% 3+	75% 2+	75% 3+
10	2/M	Positive	90% 3+	90% 3+	90% 3+
11	2/M	Positive	90% 2+	90% 3+	90% 3+

Conclusions: NGFR IHC correlated with *BCOR* ITD status like that of BCOR and cyclin D1 IHC, but demonstrated superior specificity, PPV and NPV, but the number of tumors in the comparison group were small. However, NGFR is of clinical utility in supporting the diagnosis of CCSK when used in concert with BCOR and cyclin D1 IHC.

1791 Infantile inflammatory myofibroblastic tumors (IMT): A multi-institutional study

Oscar Lopez Nunez[1], Ivy John[2], Ryane Panasiti[3], Sarangarajan Ranganathan[4], Lea F. Surrey[3], Luisa Santoro[5], Diane Grélaud[6], Rita Alaggio[2]

[1]UPMC Children's Hospital of Pittsburgh, Bethel Park, PA, [2]University of Pittsburgh Medical Center, Pittsburgh, PA, [3]The Children's Hospital of Philadelphia, Philadelphia, PA, [4]UPMC Children's Hospital of Pittsburgh, Pittsburgh, PA, [5]Azienda Ospedaliera Padova, Padova, Italy, [6]University and Regional Laboratories, Region Skåne, Malmö, Sweden

Disclosures: Oscar Lopez Nunez: None; Ivy John: None; Ryane Panasiti: None; Sarangarajan Ranganathan: None; Lea F. Surrey: None; Luisa Santoro: None; Diane Grélaud: None; Rita Alaggio: None

Background: IMT are locally aggressive, rarely metastasizing myofibroblastic neoplasms that primarily occur in children and adolescents. IMT in the first year of life are rare and poorly investigated. 4 infantile omental IMT carrying an ALK-1 inversion and 2 pulmonary IMT resembling fetal lung interstitial tumor with an A2M-ALK rearrangement were recently reported. Our aim is to explore clinicopathologic and molecular features of IMT in the first year of life.

Design: 130 pediatric IMT were retrieved from institutional and consultation archives from 3 large pediatric institutions. H&E stained slides and available immunostains from patients less than 12m of age were reviewed. ALK-1 immunostains when not available were newly performed. Results from molecular studies and/or FISH for ALK-1 were reviewed.

Results: 12 out of 130 IMT occurred in children less than 1yr. 3 were reclassified as inflammatory pseudotumors and lipoblastoma. The mean age was 5.5m, with an M:F ratio of 5:4. The location was: intestinal/mesenteric (6), head/neck (2), and adrenal gland (1). 7 IMT were hypocellular and showed a myxoid pattern with perivascular condensation of stellate to ovoid cells with thin cytoplasmic rim dispersed in a myxoid stroma containing lymphocytes and eosinophils. Collagenized stroma with focal cellular areas was dominant in 2. All cases showed a prominent vascular network with arterioles surrounded by onion-skin fibrosis/hyalinosis with 2 cases even mimicking a vascular tumor. Classic IMT morphology with minimal myxoid stroma and diffuse cytoplasmic ALK staining was seen in 2 (6m, adrenal; 8m, abdominal). In contrast, the 7 myxoid vascular IMT showed a single cytoplasmic dot-like or diffuse granular ALK-1 staining in 3 and 4 cases, respectively. ALK-1 FISH analysis in 4 myxoid vascular IMT showed an inversion with 2 of them harboring an EML4 partner gene by next-generation sequencing. No recurrences were documented in 7 cases with follow-up.

Conclusions: 7% of pediatric IMT can arise within the first year of life and may simulate other mesenchymal or vascular lesions. They are more frequent in the abdomen. Histologically they show a peculiar hypocellular myxoid vascular pattern and are often associated with dot-like/granular ALK-1 staining and ALK-EML4 rearrangement (2/2 of tested cases). These lesions resemble the omental mesenteric hamartoma described by Gonzales-Crussi and may represent the infantile variant of IMT. Awareness of this peculiar morphology is important to prevent misdiagnoses.

1792 Pleomorphic Xanthoastrocytoma with Anaplastic Features: Reevaluation of the Criteria of Malignancy in 7 Pediatric Cases

Fabiana Lubieniecki[1], Gabriela Lamas[2], Veronica Solernou[3], Valeria Vazquez[4]
[1]Hospital de Pediatria J.P.Garrahan, Buenos Aires, Argentina, [2]Buenos Aires, Argentina, [3]Hospital Garrahan, Villa Ballester, Argentina, [4]Hospital de Pediatría J.P. Garrahan, Buenos Aires, Argentina

Disclosures: Fabiana Lubieniecki: None; Gabriela Lamas: None; Veronica Solernou: None; Valeria Vazquez: None

Background: Pleomorphic xanthoastrocytoma (PXA) is an uncommon tumor accounting less than 1% of all astrocytic neoplasms. It was first described by Kepes in 1979 as an entity with clinicopathologic features of a glial tumor of pleomorphic appearance with a variable neuronal expression and a favorable clinical behavior. Subsequently, aggressive cases have been described. Nevertheless, only recently in the WHO 2016 classification, criteria for anaplastic PXA (A-PXA) have been established. The association with epithelioid glioblastoma is still uncertain.

Design: From the 2005-2018 hospital database we identified pediatric PXA cases with findings of anaplasia in the report: presence of mitosis, necrosis, and/or elevated Ki-67 expression. The current criteria (WHO 2016) were reevaluated considering morphological findings in biopsies of primary and recurrent tumors and molecular studies were performed.

Results: Seven cases were included; four were female. Mean age at presentation was 9 years (range, 2 to 12 years). All the tumors were hemispheric, involving the temporal lobe in 6 of 7 cases. Three of 7 patients underwent more than one biopsy because of tumor recurrence. One patient was diagnosed as having astrocytoma 7 years previously. Pathology findings: Protein granules were identified in 6 /7, lymphocytic infiltrates in 7/7, presence of mitosis in 7/7, of more than 5 in 10 HFP in 5/7 in the initial or relapse biopsy. In two cases increased mitosis was observed between the initial biopsy and the biopsy after relapse (4 to 15 in 10 HPF). Necrosis was observed in 3/7 cases, at the 5th relapse in one. Ki67 was elevated (>10%) in 5/5. Evaluation for BRAF V600E was performed in 5 cases, and was positive in 4/4 that could be assessed. Five of 7 patients died during follow-up, one patient is alive, and outcome is unknown in the remaining case.

Conclusions: Isolated cases of A-PXA have been described, although no case series have been reported in children. Tumor behavior in our cases shows that any of the pathological findings described in this study may be associated with a malignant prognosis. We consider that, although the mitotic index is the criterion of established anaplasia, necrosis and proliferative index should also be taken into account individually for the follow-up and adequate clinical management.

1793 Dedifferentiation in SDH-Deficient Gastrointestinal Stromal Tumor: A Report of the First Case

Faizan Malik[1], Teresa Santiago[2], Armita Bahrami[3], Eric Davis[3], Beth McCarville[2], Scott Newman[3], Elizabeth Azzato[2], Andrew Davidoff[3], Rachel Brennan[3], David Ellison[2], Michael Clay[2]
[1]University of Tennessee Health Science Center, Memphis, TN, [2]St. Jude Children's Research Hospital, Memphis, TN, [3]St. Jude Children's Research Hospital, Memphis, TN

Disclosures: Faizan Malik: None; Teresa Santiago: None; Armita Bahrami: None; Eric Davis: None; Beth McCarville: None; Scott Newman: None; Elizabeth Azzato: None; Andrew Davidoff: None; Rachel Brennan: None; David Ellison: None; Michael Clay: None

Background: Dedifferentiation in gastrointestinal stromal tumor (GIST) is a rare histologic change which may occur de novo or secondary to Imatinib therapy. Most GISTs harbor activating mutations in *KIT* or *PDGFRA*, with the remaining "wild type" GISTs predominately containing loss of function variants in the succinate dehydrogenase genes. Most SDH-deficient GISTs are pediatric gastric tumors, have epithelioid cytomorphology, and have a predilection for nodal metastasis. We describe the first case of a dedifferentiated GIST with a confirmed *SDHB* mutation.

Design: An 18-year-old male presented with a large abdominal mass of unknown etiology. Exploratory laparotomy revealed a 23.0 cm mass arising from the wall of the stomach. The tissue was routinely processed for histological, immunohistochemical, flow cytometric and molecular analysis.

Results: Two microscopic patterns of growth were identified. The first was well-differentiated (WD) and composed of sweeping fascicles of bland spindled cells with pale nuclei and prominent perinuclear cytoplasmic vacuolization. The mitotic rate was 2 mitoses per 5 mm^2. The second pattern was dedifferentiated (DD), consisting of sheets of discohesive cells with a spectrum of rhabdoid, epithelioid, and plasmablastic cytomorphologies. The DD component showed prominent nucleoli, marked pleomorphism, and brisk mitotic activity with atypical forms (26 mitoses per 5 mm^2). Immunohistochemically, the tumor showed diffuse staining for DOG-1, CD117, and CD34 in the WD component and complete absence of staining in the DD foci. SDH-B staining was negative in both components with positive internal controls (Figure 1). P53 and Ki-67 staining were diffusely positive in the DD component. Whole exome and transcriptome analysis in both components revealed an *SDHB* splice site alteration (c.286G>A; p.Gly96Ser) with evidence of loss of heterozygosity (LOH). In addition, the DD component harbored additional single nucleotide variants (41 vs. 11 in WD), copy number variations, and segments of LOH (Figure 2).

Figure 1 - 1793

Figure 1: Features of SDH-Deficient GIST with Dedifferentiation

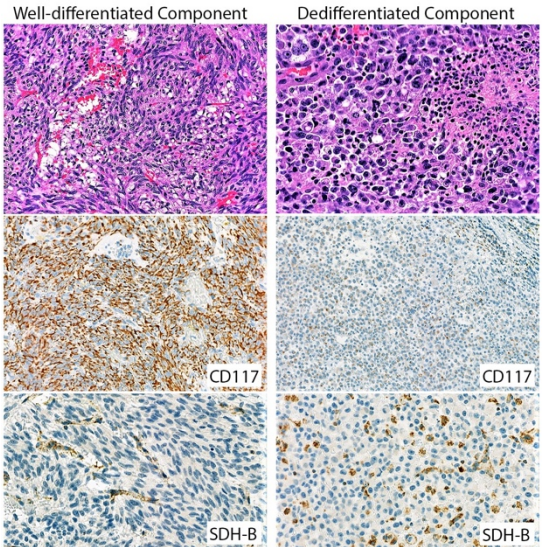

Figure 2 - 1793

Figure 2: Circos plots displaying copy number changes (outer track) and loss of heterozygosity (LOH, inner track) in well-differentiated and dedifferentiated components of GIST

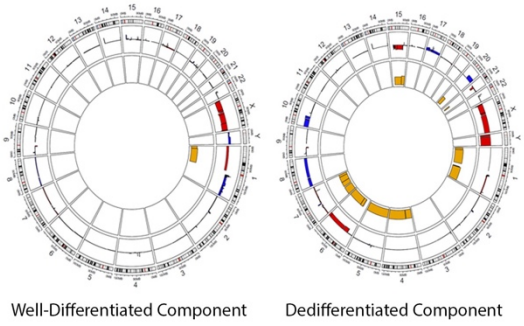

Well-differentiated component showing few copy number abnormalities including LOH of chromosome 1p (containing SDHB, 1p36.13). Dedifferentiated component showing greater copy number abnormalities including segmental chromosomal losses and gains, as well as more frequent LOH events.

Conclusions: Dedifferentiation in GIST is characterized by areas of well-differentiated GIST adjacent to a subclonal process with anaplastic morphology and a phenotypic shift. The differential diagnosis is often wide and includes non-mesenchymal tumors such as high-grade lymphoma and melanoma. SDH-deficient GISTs are more common in the pediatric setting, and no previous known cases of dedifferentiation have been reported. Herein we describe the first case with a confirmed *SDHB* alteration.

1794 Tumor Mutational Burden in Wilms Tumor (WT): A Pilot Study

Aidas Mattis[1], Latisha Love-Gregory[2], Samantha McNulty[3], John Pfeifer[3], Louis Dehner[2], Mai He[2]
[1]St. Louis, MO, [2]Washington University School of Medicine, St. Louis, MO, [3]Washington University, St. Louis, MO

Disclosures: Aidas Mattis: None; Latisha Love-Gregory: None; Samantha McNulty: None; John Pfeifer: None; Louis Dehner: None; Mai He: None

Background: WT is the most common renal neoplasm in children. However, about 10%-15% of patients respond poorly to current therapy. To-date, anaplasia is the only major histologic prognostic indicator for treatment response and 50% of patients identified with anaplasia in WT are expected to recur. Our group previously reported that a small percentage of WTs stain positive for PD-L1 & PD-1 immunohistochemistry. Here we examine tumor mutational burden (TMB) in WTs with various features including metastasis, anaplasia, and syndromic, for potential response to checkpoint blockade immunotherapies.

Design: WT cases (n=7, 4 males & 3 females; aged 2-8 y/o) were identified from departmental archives from 2000 to 2017. Genomic DNA was extracted from FFPE tissue of normal and tumor tissue. Whole exome sequencing was performed on the Illumina HiSeq3000 platform for tumor and non-tumor at a depth of 25-30 M reads for normal and 45-50 M reads for tumor. Variants were called by VarScan2 down to an allele frequency of 1%. The processSomatic command from varscan was used to identify somatic variants, including high confidence variant calls. The high confidence SNPs and indels were totaled and divided by 54 Mb, the size of the exome target region, to obtain the tumor mutation load.

Results: Two specimens showed markedly increased TMB: 2.28 and 18.7, for sporadic with anaplasia and syndromic without anaplasia, respectively. Both patients had received chemotherapy prior to surgery. The remainder of the sequenced specimens TMB ranged from 0.61 to 1.76, showing no clear trend when comparing the various groups of syndromic, anaplasia, or metastases. One other patient had treatment prior to surgery with a TMB of 0.94. Two metastases were compared to their respective primary lesions and the mutational burden was slightly increased by 0.08 in the metastasis from the sporadic case and decreased in the metastasis from the syndromic case (1.76 versus 1.07), showing no clear correlation.

Conclusions: Whole exome sequencing showed variable mutation burden in WT, including markedly increased TMB in two of seven (28.6%) patients suggesting potential benefit from checkpoint blockade therapy. As these two were both patients who received treatment, treatment cannot be ruled out as the cause for the increase in TMB. Future work includes checking DNA mismatch repair and hypermutation genes for mutations and most importantly, a larger study is needed.

1795 Adult-Type Cancers Happen in Children Too: A Retrospective Review of Three Adolescent Patients with Isocitrate-Dehydrogenase-1 (IDH1) Mutated Brain Tumors

David Metter[1], Ameet Thaker[2], Sandy Cope-Yokoyama[3], Dinesh Rakheja[4], Veena Rajaram[5]
[1]University of Texas Southwestern, Dallas, TX, [2]UT Southwestern/Children's Health Dallas, Dallas, TX, [3]Fort Worth, TX, [4]University of Texas Southwestern Medical Center, Dallas, TX, [5]Children's Health/UT Southwestern Medical, Dallas, TX

Disclosures: David Metter: None; Ameet Thaker: None; Sandy Cope-Yokoyama: None; Dinesh Rakheja: None; Veena Rajaram: None

Background: Isocitrate-dehydrogenase (IDH) enzymes, IDH1-3, catalyze the decarboxylation of isocitrate to ?-ketoglutarate. *IDH1* and *IDH2* mutations are common in adult gliomas and confer a favorable prognosis. The mutant IDH enzymes drive overproduction of D-2-hydroxyglutarate that can be detected in vivo by magnetic resonance spectroscopy. Small molecule inhibitors of mutant IDH have emerged as therapeutic options and are in clinical trials. IDH mutated gliomas are rare in children, but their recognition is important because of prognostic, diagnostic, and therapeutic implications.

Design: Retrospective review of 3 pediatric cases of IDH1 mutated gliomas occurring at a single institution was conducted using the electronic health records, pathology reports, and H&E and IHC glass slides. Immunohistochemsitry for IDH1 R132H mutation was performed due to histologic features atypical from the usual pediatric gliomas such as pilocytic astrocytoma (PA), dysembryoplastic neuroepithelial tumor (DNET), and ganglioglioma.

Results: From 2011 to 2018, 3 IDH1 mutated gliomas with unusual histology for pediatric gliomas were identified at our institution in patients ranging from 11-18 years old. The first case of IDH1 mutated diffuse astrocytoma (DA) was diagnosed in an 11-year-old boy with monthly headaches and a right frontal lobe subcortical mass on magnetic resonance imaging. A second IDH1 mutated DA was diagnosed in a 16-year-old boy with new-onset headaches and seizures with a left frontal lobe mass on computerized tomography scan; fluorescence in situ hybdridization was negative for *1p/19q* co-deletion. The third case was diagnosed as IDH1 mutated, *1p/19q* co-deleted oligodendroglioma (OG) in an 18-year-old girl with new-onset seizures and a non-enhancing left parietal cortical mass on magnetic resonance imaging.

Conclusions: For pediatric gliomas, DA is a much less common histologic type than PA. Likewise, OG is much rarer than DNET. Our cases highlight the importance of testing for IDH mutation with reflex to *1p/19q* co-deletion in unusual histology gliomas in pediatric patients, particularly those occurring in adolescence.

1796 Pediatric Post Transplant Lymphoproliferative Disorder Identified on Random Gastrointestinal Biopsies Show Non-Mass Forming PTLD with Clonal B-Cells and Plasma Cells: Report of 3 Cases

Alia Nazarullah[1], Hamza Tariq[1], Cynthia Forker[2], Kenneth Holder[3]
[1]The University of Texas Health Science Center at San Antonio, San Antonio, TX, [2]San Antonio, TX, [3]The University of Texas Health Science Center at Houston, San Antonio, TX

Disclosures: Alia Nazarullah: None; Hamza Tariq: None; Cynthia Forker: None; Kenneth Holder: None

Background: EBV related lymphoproliferations in post transplant settings range from non-destructive hyperplasia to polymorphic post transplant lymphoproliferative disorder **(**PTLD) to overt lymphoma. Here we present three cases of pediatric gastrointestinal (GI) PTLDs, identified on random biopsies due to vague gastrointestinal symptoms (diarrhea, abdominal pain and food intolerance) with hypoalbuminemia. The cases are non-mass forming and non-destructive, but showed focal polymorphic appearing lymphoid infiltrate with EBV positivity, monotypic plasma cells and clonal B-cells.

Design: An electronic search for pediatric PTLDs with GI involvement yielded three cases. Chart review for clinical and imaging findings was performed. Immunohistochemical stains (IHC) and EBER ISH were performed on formalin fixed paraffin embedded tissue. PCR for IGH and/or IGK gene rearrangements were performed in 2/3 cases. Flow cytometry on ascitic fluid and bone marrow was performed on 1/3 cases.

Results: All children were EBV-naive and presented within 1 year of transplant with vague abdominal symptoms. Clinical findings included cytopenia (3 of 3 cases), hypoalbuminemia (3 of 3 cases) and EBV viremia (3 of 3 cases). Upper and lower GI endoscopies did not reveal any mass lesions. A focal non-destructive polymorphic lymphoid infiltrate was identified on random GI biopsies. All cases showed a polymorphic lymphoid infiltrate admixed with plasma cells and many EBV positive cells. Plasma cells were light chain restricted by IHC in 2/3 cases. 1 case showed involvement of ascitic fluid and bone marrow, with light chain restricted plasma cells detected by flow cytometry. Cyclophosphamide, steroids and Rituximab treatment had good clinical response in all cases, including one case which had incomplete response with Rituxan alone. See Table 1.

Summary of non-mass forming pediatric GI PTLD cases								
Case	**Age/Ethnicity**	**Transplant history**	**Symptoms/Clinical findings**	**Serum EBV**	**Endoscopic/imaging findings**	**Site of lesion**	**IHC/flow cytometry**	**Molecular studies**
1	18 mths, Hispanic	Liver transplant for biliary atresia	Diarrhea, low albumin, pancytopenia	2529 copies/mL	Unremarkable, no mass lesions	Duodenum	Kappa restricted plasma cells	Positive for clonal IGH rearrangement
2	23 mths, Hispanic	Liver transplant for biliary atresia	Diarrhea, lethargy, ascites, low albumin, anemia	722406 copies/mL	Unremarkable, no mass lesions	Duodenum	Lambda restricted plasma cells	Positive for clonal IGH and IGK rearrangements
3	6 years, African-American	Kidney transplant for diffuse mesangial sclerosis	Diarrhea, low albumin, leukopenia	14212 copies/mL	Unremarkable, no mass lesions	Ascending colon	Lambda restricted plasma cells	Not performed

- **Conclusions:** Gastrointestinal PTLD in children can present within one year of transplant with vague abdominal symptoms, cytopenia and hypoalbuminemia, and can be non-mass forming and non-destructive; high level of suspicion with random GI biopsies are recommended.
- These cases show morphologic features of early/non-destructive lesions but have clonal B-cells and/or plasma cells, suggestive of a polymorphic PTLD type process.
- These cases seem to have a better response to chemotherapy than Rituximab alone.
- Since these patients have no mass lesions, clinical improvement, EBV viral load, improvement in cytopenia and serum albumin levels may be used for response to therapy.

1797 High-Risk Histopathologic Features Analysis of Primary Enucleated Retinoblastoma in Tanzania Patients

Claire Ndayisaba[1], Dianna Ng[2], Edda Vuhahula[1], James Kitinya[3]
[1]Muhimbili University of Health and Allied Sciences, Dar es Salaam, Tanzania, [2]UCSF Medical Center, San Francisco, CA, [3]United Nations Road, Dar es Salaam, Tanzania

Disclosures: Claire Ndayisaba: None; Dianna Ng: None; Edda Vuhahula: None; James Kitinya: None

Background: The presence of high-risk histopathologic features in retinoblastoma, namely, massive choroid infiltration, post-laminar optic nerve invasion, scleral invasion, and evidence of extraocular tumor, including positive optic nerve margin, and extrascleral extension, in an enucleated eye specimen is an indication for adjuvant chemotherapy. The aim of this study is to evaluate the prevalence of high-risk histopathologic features in enucleated eye specimens for retinoblastoma in Tanzania, and to determine if there is a correlation between high-risk features with clinical findings.

Design: A retrospective review of enucleation specimens for retinoblastoma from 1/1/2013-12/31/2016 was performed at our institution. Demographic, clinical and histopathologic data were collected, including age, gender, family history of retinoblastoma, initial sign/symptom, duration between onset of sign/symptom to surgery, international classification of retinoblastoma (ICRB) group classification, tumor growth pattern, tumor extension and pathologic grade and stage, according to the American Joint Committee on Cancer. Relationship between age, gender, symptom duration, ICRB group, tumor growth pattern and the need for adjuvant therapy were evaluated.

Results: 132 patients were identified (median age 33 months, range 3-108 months, 68 male, 64 female). Bilateral disease was noted in 23/132 participants (17.4%). Leukocoria was the predominant clinical presentation in 92/132 (69.7%). The mean interval between onset of clinical symptoms and surgery was 11 months. Eight two of 132 participants (62%) were in clinical stage group E. One or more high-risk histopathologic features were noted in 83/132 participants (63%). Massive choroid invasion alone was recorded in 13/83 cases (16%). Postlaminar optic nerve invasion was in seen in 5/83 cases (6.0%). Partial scleral invasion was noted in 8/83 cases (9.6%). Evidence of extraocular tumor, including positive optic nerve margin and extrascleral invasion, was the most common high risk feature and was noted in 57/83 cases (68.6%). A statistically significant association was noted between the need for adjuvant therapy and a symptom duration period of >6 months, clinical group E and both mixed and exophytic tumor growth patterns by both univariate and multivariate regression analyses.

Conclusions: The frequency of high-risk histopathologic features in enucleated eye specimens in Tanzania is high. Although advanced clinical presentation is associated with the presence of high-risk features

1798 Liposarcoma In Children and Young Adults: A Clinicopathologic and Molecular Study of 23 Cases

Ran Peng[1], Nan Li[2], Huijiao Chen[3], Min Chen[1], You Xie[1], Zhang Zhang[3], Ting Lan[1], Wei Zhao[1], Hongying Zhang[3]
[1]West China Hospital, Sichuan University, Chengdu, China, [2]The Fourth Hospital of Harbin Medical University, Pathology Department, Harbin, China, [3]Chengdu, China

Disclosures: Ran Peng: None; Nan Li: None; Huijiao Chen: None; Min Chen: None; You Xie: None; Zhang Zhang: None; Ting Lan: None; Wei Zhao: None; Hongying Zhang: None

Background: Liposarcoma represents the most common mesenchymal malignant tumors of adults. However, liposarcoma in young patients before 22 years of age is extremely rare and the majority of published cases lack molecular confirmation. The authors present the largest series in an Asian population.

Design: Between January 2007 and September 2018, 23 cases younger than 22 years of age were included. This series of liposarcoma accounted for 2.4% of all the liposarcomas during the same period. The clinicopathologic features of all cases were reviewed. Amplification of *MDM2* and/or rearrangement of *DDIT3* fluorescence *in situ* hybridization (FISH) and polymerase chain reaction for *Tp53* mutation were performed on tumors with enough materials.

Results: This series included 15 females and 8 males (M: F=1:1.9) ageing from 7 to 22 years of age (median 17.0 y, mean 17.1 y). Tumors occurred mainly in the lower extremities (14/23, 61%), followed by trunk (5/23, 22%), head/neck (2/23, 9%) and arm/retroperitoneum (2/23, 9%). The median tumor size was 8 cm (range 4-28 cm). The tumors were classified as the following subtypes: myxoid liposarcoma (MLPS, n=16), atypical lipomatous tumor/well-differentiated liposarcoma (ALT/WDL, n=3), dedifferentiated liposarcoma (DDL, n=1), and pleomorphic liposarcoma (PLPS, n=3). The tumors were graded as French Federation of Cancer Centers (FNCLCC) grade 1 (74%), grade 2 (17%), and grade 3 (9%). FISH was performed on 18 cases. *MDM2* amplification was detected in all 4 ALT/WDL/DDL. All 12 MLPS showed *DDIT3* rearrangement. Both two tested PLPS showed in absence of *DDIT3* and/or *MDM2* variation but harbored *Tp53*mutation. All 23 patients underwent surgical operation, and 6 of them received adjuvant therapy. Seventeen patients were available for follow-up information with a median duration of 21 months (range 2-108 mo). Fifteen patients were alive with no evidence of disease (range 2-94 mo; median 20 mo). One patient with retroperitoneal WDL developed multiple recurrences and was alive with disease for 108 months. One patient with PLPS in chest wall developed metastasis and died of disease at 43 months.

Conclusions: This study suggests that liposarcoma occurring in young children is extremely rare but do exist. MLPS seems to be the most common subtype, followed by ALT/WDL, PLPS, and DDL. Additional cases are needed to identify and determine whether the clinicopathological features and molecular pathogenesis differ in pediatric and adult populations.

1799 Sertoli-Leydig Cell Tumors: a Morphologic Study of 9 Female Pediatric Cases

Amanda Strickland[1], Hao Chen[2], Dinesh Rakheja[1]
[1]University of Texas Southwestern Medical Center, Dallas, TX, [2]Coppell, TX

Disclosures: Amanda Strickland: None; Hao Chen: None; Dinesh Rakheja: None

Background: Sertoli-Leydig cell tumor is a distinct sex cord stromal ovarian neoplasm that comprises less than 0.5% of ovarian neoplasms, and primarily affects children and young adults. Recently, DICER1 mutations have been shown to characterize Sertoli-Leydig cell tumors particularly those of intermediate to poor differentiation. Thus, a morphologic diagnosis of this rare tumor may have implications for germline genetic screening to assess for DICER1 syndrome in children presenting with an ovarian tumor. Here, we present the histopathologic features of 9 female pediatric Sertoli-Leydig cell tumors.

Design: A search of the pathology report database at a large metropolitan children's hospital retrieved 9 cases diagnosed as Sertoli-Leydig cell tumor. H&E stained slides and completed immunohistochemical studies were reviewed. Basic patient demographics and morphologic features were recorded and compared.

Results: The age at presentation ranged from 6 to 15 years, with mean of 12.9 years, median 14 years, and mode 14 years. The primary tumor size ranged from 1 to 27 cm, with a mean of 14 cm and median of 13 cm. Microscopically, 100% (9/9) of the cases showed intermediate to poor differentiation. A heterologous component was present in 67% (6/9) of the cases; rhabdomyosarcoma and adenocarcinoma were both identified in 2 cases (22%, 2/9). 22% (2/9) cases contained retiform features. 89% (8/9) cases contained multiphasic architecture; the architectural patterns included sheets (67%, 6/9), cords and trabeculae (44%, 4/9), cysts (22%, 2/9), nodules (22%, 2/9) and tubular structures (22%, 2/9). Necrosis was identified in 33% (3/9) cases.

Conclusions: Sertoli Leydig cell tumor is rare in the pediatric gynecology population. This study highlights the unique histopathologic properties in female pediatric cases.

1800 CHD5 Expression Profile as a Potential Marker for Early Assessment of Response to Treatment in High-Risk NB

Mariona Sunol[1], Soledad González[1], Carlota Rovira[2], Crisitna Jou[2], Silvia Planas[2], Sara Perez-Jaume[2], Teresa Ribalta[3], Eva Rodriguez[2], Ofelia Cruz[4], Jaume Mora[1], Cinzia Lavarino[5]
[1]Hospital Sant Joan de Deu, Esplugues de Llobregat, Spain, [2]Hospital Sant Joan de Deu, Barcelona, Spain, [3]Barcelona Children's Hospital Sant Joan de Deu, Esplugues de Llobregat, Spain, [4]Sant Joan de Deu, Barcelona, Spain, [5]Barcelona, Spain

Disclosures: Mariona Sunol: None; Soledad González: None; Sara Perez-Jaume: None; Teresa Ribalta: None

Background: In Neuroblastoma (NB), low/absent expression of CHD5 at diagnosis is strongly associated with unfavorable clinico-biological features. Our previous findings highlighted the existence of a subset of high-risk NBs that acquire CHD5 expression following chemotherapy. CHD5 expression was associated with disease response to cytotoxic induction therapy and subsequently with overall survival (OS). Here, we investigated CHD5 expression as a potential marker for early assessment of response to treatment in patients with NB.

Design: A total of 36 NB patients treated in our institution between 2007-2017 were included in the study. Eligible patients included previously untreated, stage 4 NB (INSS), and non-stage 4 *MYCN* amplified tumors. Patients were treated according to N7-induction protocol (MSKCC). Immunohistochemical analysis was performed on paired diagnostic and second-look biopsies (following cycle 3 of induction) using anti-CHD5 and anti-Ki-67 antibodies. Percentage of positive cells and nuclear staining intensity was recorded. Survival curves were performed using the Kaplan-Meier method and compared with log-rank test.

Results: Negative/weak CHD5 immunostaining and a high percentage of Ki-67 positive (range 50-90%) tumor cells was observed in all tumors at the moment of diagnosis. At second-look, CHD5 positive staining was observed in 21/36 (58%) tumors, together with clear therapy-induced morphological changes (increased cytoplasm) and a decrease of the percentage Ki-67 positive (range 5-30%) cells. At time of analysis, 16/21 (76%) patients were alive, median follow-up for alive patients of 92 months. Negative CHD5 expression persisted in 15/36 (42%) tumor biopsies, along with only minor morphological changes. At analysis, 3/15 (20%) patients were alive, median survival of 33 months. CHD5 expression profile was compared to overall and event-free survival (EFS) and was found to be significantly associated with OS (P<0,0001) and EFS (P<0,0001).

Conclusions: Findings suggest the existence of a subset high-risk NB where CHD5 expression is restored in response to chemotherapy. Therapy-induced CHD5 expression is associated with longer OS and EFS, and with enhanced response to cytotoxic therapy. CHD5 immunohistochemical expression profile is a potential surrogate marker for early assessment of response to treatment that can be useful for **identifying patients that do not benefit from established high-risk treatment and need novel treatment strategies.**

1801 INSM1 Expression in Peripheral Neuroblastic Tumors and Other Pediatric Small Round Blue Cell Neoplasms

Hannah Wang[1], Chandra Krishnan[2], Greg Charville[1]
[1]Stanford University School of Medicine, Stanford, CA, [2]Dell Children's Medical Center, Austin, TX

Disclosures: Hannah Wang: None; Greg Charville: None

Background: Insulinoma-associated protein 1 (INSM1) is a transcription factor that functions in the neuroepithelial tissue development and shows expression in neuroendocrine neoplasms. Given the role of INSM1 in controlling differentiation of the sympatho-adrenal lineage, we hypothesized that INSM1 expression would define a subset of neuroblastic tumors. This study aims to characterize the immunohistochemical profile of INSM1 in a cohort of peripheral neuroblastic tumors, and compare INSM1 expression in these tumors to that seen in other small round blue cell neoplasms.

Design: We evaluated 73 tumors using a tissue microarray, including 37 peripheral neuroblastic tumors, 14 rhabdomyosarcomas, 13 nephroblastomas, and 9 Ewing sarcomas. An additional 7 peripheral neuroblastic tumors were evaluated for INSM1 expression on whole-slide sections. Immunohistochemical studies for INSM1, synaptophysin, and chromogranin were performed on 4-mm, formalin-fixed paraffin-embedded sections. Cases were considered positive for INSM1 expression when 1% or more of tumor nuclei were immunoreactive, and positive for synaptophysin and chromogranin when 5% or more of tumor cell cytoplasm was immunoreactive.

Results: INSM1 staining was not as sensitive or specific as synaptophysin or chromogranin for neuroblastoma among small round blue cell tumors. A total of 34/44 (77%) peripheral neuroblastic tumors were positive for INSM1 expression (Table 1 and Figure 1). Five patients had paired pre- and post-treatment tumors. Three patients had INSM1 negative tumors which became INSM1 positive after treatment.

Table 1. Comparison of INSM1 to Other Markers of Neuroendocrine Differentiation

	INSM1	Synaptophysin	Chromogranin
Peripheral Neuroblastic Tumor	34/44 (77%)	36/37 (97%)	33/37 (89%)
Neuroblastoma	25/32 (78%)	28/29 (97%)	25/29 (86%)
Ganglioneuroblastoma	9/9 (100%)	7/7 (100%)	7/7 (100%)
Ganglioneuroma	0/3 (0%)	1/1 (100%)	1/1 (100%)
Ewing Sarcoma	1/9 (11%)	0/9 (0%)	0/9 (0%)
Rhabdomyosarcoma	8/14 (57%)	2/14 (14%)	1/14 (7%)
Nephroblastoma	4/13 (31%)	1/13 (8%)	0/13 (0%)

Figure 1 - 1801

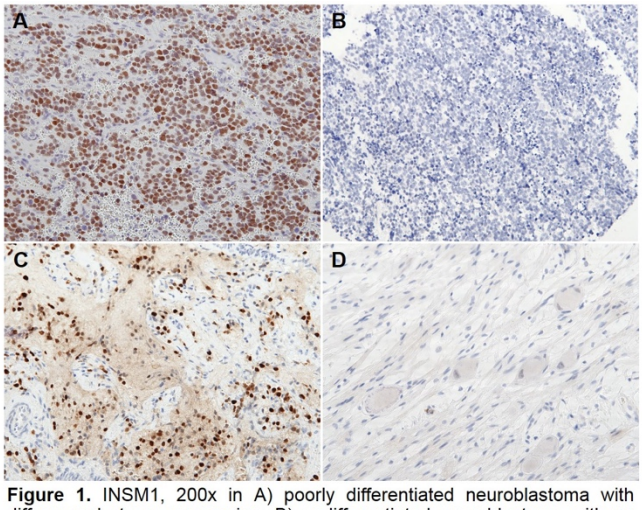

Figure 1. INSM1, 200x in A) poorly differentiated neuroblastoma with diffuse and strong expression, B) undifferentiated neuroblastoma with no expression, C) ganglioneuroblastoma with variable expression, and D) ganglioneuroma with no expression.

Figure 2 - 1801

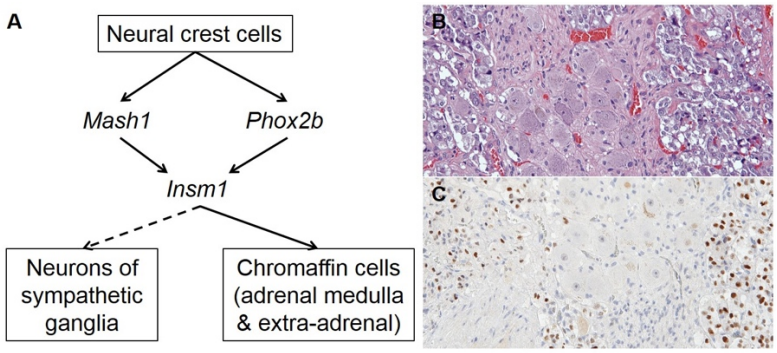

Figure 2. A) Schematic of sympatho-adrenal differentiation adapted from Wildner et al. 2008. *Insm1* functions downstream of *Phox2b* and *Mash1* in sympatho-adrenal differentiation. Its expression is seen in mature chromaffin cells but not in mature ganglion cells as demonstrated in panels B) H&E, 200x, and C) INSM1, 200x.

Conclusions: Our findings suggest that INSM1 staining is a non-specific marker of neuroblastoma in the pediatric population. INSM1 expression was identified in a subset of neuroblastomas, all ganglioneuroblastomas, and no ganglioneuromas. This contrasts with other markers of neuroendocrine differentiation, such as synaptophysin and chromogranin. These findings suggest that INSM1 expression may reflect neuroblastic tumor involution/maturation, in keeping with its role in controlling later steps of sympatho-adrenal differentiation (Figure 2). While no significant differences in INSM1 staining were seen between undifferentiated, poorly differentiated, and differentiating histologic subtypes of neuroblastoma, our study may not be powered to detect this difference. Additional studies are needed to determine whether INSM1 expression is indicative of a clinically significant differentiation state in neuroblastoma.

1802 Dermatofibrosarcoma Protuberans in Chinese Pediatric Patients: Clinicopathologic Features and Cytogenetic Analysis of 33 Cases

Zhang Zhang[1], Min Chen[2], Huijiao Chen[1], Hongying Zhang[1]
[1]Chengdu, China, [2]West China Hospital, Sichuan University, Chengdu, China

Disclosures: Zhang Zhang: None; Min Chen: None; Huijiao Chen: None; Hongying Zhang: None

Background: Dermatofibrosarcoma protuberans (DFSP) is one of the most common dermal sarcomas in adult, but it is rare in childhood. The clinical appearance may be more difficult to identify and likely misdiagnosed or underdiagnosed than adults. The authors present the clinical application value of *COL1A1-PDGFB* fusion gene detection by fluorescence in situ hybridization (FISH) in the largest series of pediatric cases of DFSP in Asia population.

Design: Pathology files of West China Hospital Sichuan University diagnosed of DFSP younger than 18 years in 2006-2017 were collected.The clinicopathologic features of all cases were reviewed. Immunohistochemical (IHC) studieswere performed: Desmin, CD34, smooth muscle actin (SMA), myogenin, S-100, p63, CD10, epithelial membrane antigen (EMA) and Ki-67. *COL1A1-PDGFB* fusion gene and *PDGFB* break-apart probe were detected by FISH analysis.

Results: Thirty-three patients were identified (mean age: 12.5years [range: 3month-17years]; 17 males, 16 females). Tumors occurred mainly in head and neck (3/33, 10%), trunk (24/33,73%) and extremities (6/33, 18%). 29 of 33 were nodular masses, and 4 of them in the plaque stage. The size of the neoplasms ranged from 1cm to 6cm(mean: 2.7cm). The tumors were classified as the following subtypes: conventional DFSPs(n=20), myxoid DFSP (n=4), sclerosing DFSP (n=1), Bednar tumor (n=2), giant cell fibroblastoma (GCF) (n=3)and fibrosarcomatous DFSP (FS-DFSP) (n=3),. In our study, the accurate histologic diagnosis of DFSP variants was more difficult than the conventional type. IHC stains showed that CD34 expression was strong and extensive in the spindle cell component in 29 of 33 (88%), including 3 cases of FS-DFSP, whereas cases of myxoid subtype had patchyor weak CD34 expression. Thirty-three samples were informative for FISH analysis. Thirty-two of 33 (97%) were *COL1A1-PDGFB* fusion signals positive with the unbalanced translocation. The break apart signal of*PDGFB*gene was detected in 31 patients (94%), except one case of GCF and one case of myxoid DFSP. Nine of 28 cases have recurred and none has metastasized.

Conclusions: For pediatric DFSP, increasing awareness amongst pediatricians and pediatric dermatologists of the clinical features, histology, genetics and treatment options is important for successful management in this neoplasm.Detection of the *PDGFB* gene rearrangement or the *COL1A1-PDGFB* fusion gene may be great useful in pediatric DFSP patients with atypical clinical presentation.